



Lawrence Berkeley National Laboratory



18 August 2017

Dear Dr. Peylin,

My co-authors and I are pleased to submit our revised manuscript titled “*Impacts of microtopographic snow-redistribution and lateral subsurface processes on hydrologic and thermal states in an Arctic polygonal ground ecosystem*” for your consideration for publication in Geoscientific Model Development.

We thank you, the executive editor, and the two reviewers for insightful and constructive feedback, which helped us to clarify important aspects of our work. Modifications made in the revised version of the manuscript as compared to initial submission are summarized below:

1. As suggestion by reviewer #1, the introduction section has been shortened by removing the description of changes in Arctic net ecosystem productivity.
2. The discussion regarding future work has been expanded to include possible approaches to parsimoniously represent fine scale processes within a global land model.
3. We added to supplementary information a description of numerical tests we performed to ensure new model developments were correctly implemented.
4. The code availability section has been revised to included reference to the publicly accessible code and dataset repositories that were used in this study.

My co-authors and I believe we have thoroughly addressed all the reviewer comments and that the revised manuscript is well suited for publication in Geoscientific Model Development. We look forward to receiving your response.

Sincerely,
Gautam Bisht

1 **Impacts of microtopographic snow-redistribution and lateral subsurface processes**
2 **on hydrologic and thermal states in an Arctic polygonal ground ecosystem [MS no.**
3 **gmd-2017-71]**

4
5 **SC1: 'Executive Editor Comment on "Impacts of microtopographic snow-**
6 **redistribution and lateral subsurface processes on hydrologic and thermal states in**
7 **an Arctic polygonal ground ecosystem"', Astrid Kerkweg**

8
9 *"The main paper must give the model name and version number (or other unique identifier)*
10 *in the title."*

11 *"If the model development relates to a single model then the model name and the version*
12 *number must be included in the title of the paper. If the main intention of an article is to make*
13 *a general (i.e. model independent) statement about the usefulness of a new development, but*
14 *the usefulness is shown with the help of one specific model, the model name and version*
15 *number must be stated in the title. The title could have a form such as, "Title outlining*
16 *amazing generic advance: a case study with Model XXX (version Y)"."*

17 **Response:**

18 We have updated the title of our manuscript to be "Impacts of microtopographic snow-
19 redistribution and lateral subsurface processes on hydrologic and thermal states in an
20 Arctic polygonal ground ecosystem: A case study using ALM-3D v1.0"

21
22 *"All papers must include a section, at the end of the paper, entitled 'Code availability'. Here,*
23 *either instructions for obtaining the code, or the reasons why the code is not available should*
24 *be clearly stated. It is preferred for the code to be uploaded as a supplement or to be made*
25 *available at a data repository with an associated DOI (digital object identifier) for the exact*
26 *model version described in the paper. Alternatively, for established models, there may be an*
27 *existing means of accessing the code through a particular system. In this case, there must exist*
28 *a means of permanently accessing the precise model version described in the paper. In some*
29 *cases, authors may prefer to put models on their own website, or to act as a point of contact*
30 *for obtaining the code. Given the impermanence of websites and email addresses, this is not*
31 *encouraged, and authors should consider improving the availability with a more permanent*

32 *arrangement. After the paper is accepted the model archive should be updated to include a*
33 *link to the GMD paper."*

34 *Inclusion of Code and/or data availability sections is mandatory for all papers and should be*
35 *located at the end of the article, after the conclusions, and before any appendices or*
36 *acknowledgments. For more details refer to the code and data policy.*

37 **Response:**

38 We have publicly released the code and data used in this study. The ALM-3D code is
39 available at <https://bitbucket.org/gbisht/lateral-subsurface-model>, while the data used in
40 this study is available at <https://bitbucket.org/gbisht/notes-for-gmd-2017-71>.

41 **RC1: 'Review of the manuscript by Bisht et al.', Anonymous Referee #1**

42

43 General comments:

44 Manuscript by Bisht et al. presents simulation results in an Arctic polygonal ground
45 ecosystem using an improved ALM model including lateral processes and snow
46 redistribution. The conclusions are partly supported by modeling results, e.g., 1) snow
47 depth variation was affected by snow redistribution, but not by lateral processes of thermal
48 flow, 2) active layer depths was affected by lateral energy fluxes. Like many others, this
49 work again stresses that advances in the land surface modeling is needed. In fact, the
50 simple snow redistribution approach in the paper can be readily incorporated into land
51 models.

52

53 *My main reservations are the selection of the 2D transect and model validation. Why the*
54 *transect is not selected where the sensors (as shown In Figure 1) are located? It makes the*
55 *comparison between the model and observation meaningless.*

56 **Response:**

57 We acknowledge that the 2D transect used for simulations in this study does not align with
58 the sensor location. The objective of this work was not to validate the model for the few
59 grid cells that exactly align with the observations recorded in the rim and center of a
60 polygon, but to quantify relative differences between simulations for rim and center of a
61 polygon. As noted in Figure 2, all grid cells above the dashed line were classified as rim,
62 while all grid cells below the dashed line were classified as center. The model accurately
63 captures the snow depth differences between rim and center when SR is turned on (Table
64 1). Additionally, errors in simulated temperature for all soil depths are lower for rim and
65 center when SR is included (Table 2). Thus, our comparison of model results against
66 observations is reasonable and the comparison we present indicates the model accurately
67 represents system characteristics important for the conclusions of our paper.

68

69 Specific comments:

70 *1) Lengthy texts in the Introduction that are not directly related to the study.*

71 **Response:**

72 We have removed text in introduction describing changes in NEP within Arctic ecosystems
73 as simulation in this work did not have an active biogeochemistry cycle.

74

75 *2) Line 100-101: define "active layer thickness" for general readers.*

76 **Response:**

77 We have added a definition for active layer thickness.

78

79 *3) Line 126: define ALM.*

80 **Response:**

81 We have updated the text to define ALM.

82

83 *4) Line 158-160: redundant as already described in lines 126-128.*

84 **Response:**

85 We have updated the text to remove redundancy.

86

87 *5) Line 169: check unit of Q .*

88 **Response:**

89 The units of Q have been corrected to [m^{-3} of water m^{-3} of soil s^{-1}]

90

91 *6) Define z in Eq. 2 and other variables in Eq. 4.*

92 **Response:**

93 All terms in Equation 2 and 4 are now defined.

94

95 *7) Eqs. 17 and 18, check the third term on the RHS.*

96 **Response:**

97 Third term in equation 17 and 18 is updated.

98

99 *8) Eq. 23: write cn as $c_{i,j,k}$*

100 **Response:**

101 In equation 23, c_n is now defined as $c_{n,i,j,k}$. Additionally, equations 25-32 have been
102 updated.

103

104 *9) Define ω' in Eqs. 25-31*

105 **Response:**

106 In equation 25-31, ω' is now replaced by $1 - \omega$, where ω is defined as the weight in the
107 Crank-Nicholson method.

108

109 *10) Line 312: from Fig. 2, I see less dependence of average snow depth on topography with
110 SR.*

111 **Response:**

112 We have fixed the typographical error and the text now reads "*With SR, a much smaller
113 dependence of winter-average snow depth on topography is predicted*"

114

115 *11) How well is the 3D model developed in the paper compared to analytical solutions or
116 other well established numerical models?*

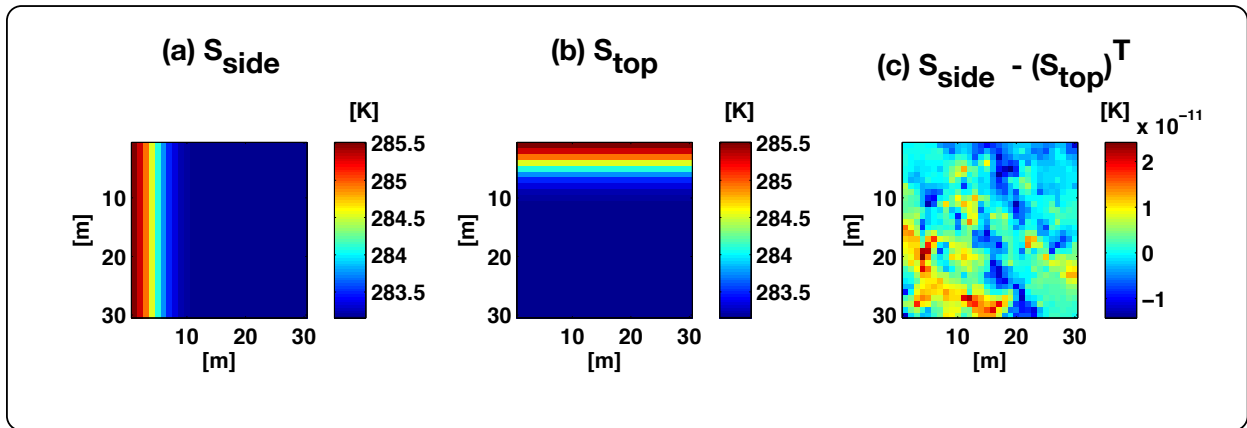
117 **Response:**

118 In this work, we extended the existing 1D physics formulations for subsurface hydrologic
119 and thermal processes to included lateral processes. Thus, we did not compare existing
120 physics formulations against analytical solutions or other numerical models, but we did
121 ensure that lateral coupling was implemented correctly. Sanity checks were preformed to
122 ensure the 3D model solution is the same as in the 1D vertical model when the problem
123 setup is horizontally homogeneous (Results not shown).

124 The thermal model is independent of gravity. Thus, additional tests were performed
125 to ensure the numerical solution of the thermal model for propagation of heat is identical in
126 a 1D column that is oriented horizontally and vertically. A test was performed to study the
127 propagation of a heat perturbation that was applied on the left and top boundary of a
128 spatially homogeneous 2D domain (Figure 1, below). The difference of simulated
129 temperature between the two cases was of the order of the tolerance of the numerical
130 solver (Figure 1c). An additional test was performed in which a sinusoidally varying

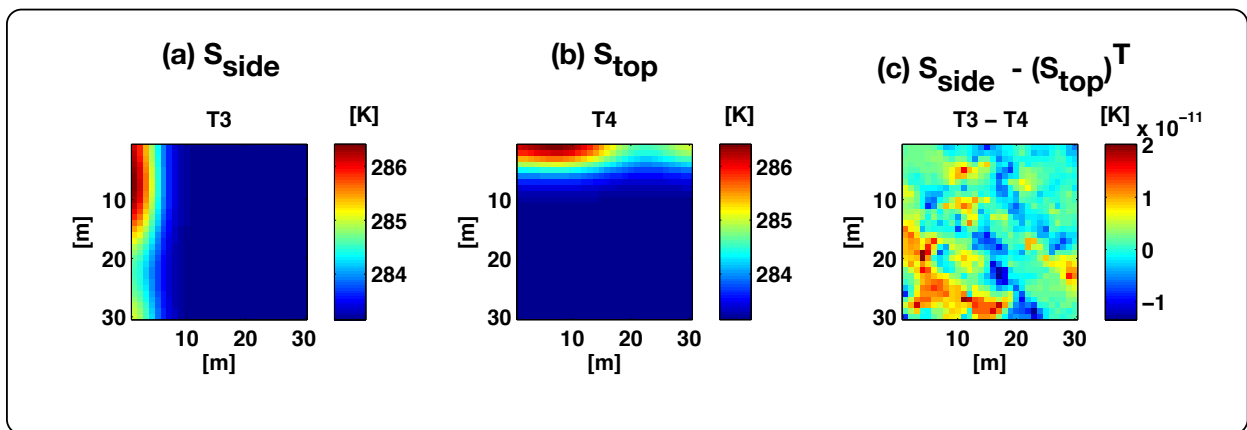
131 temperature perturbation was applied on the left and top boundary; and the difference in
 132 results was again within tolerance of numerical solver (Figure 2). These tests ensured that
 133 lateral coupling was correctly implemented within the model. To address the reviewer’s
 134 concerns regarding testing, we have added description of these analyses to the
 135 Supplementary Material (Page 2, lines 18-40, and a reference to these tests has been added
 136 to the main text (Page 12, lines 241-244).

137



138

139 **Figure 1. Propagation of a spatially homogeneous temperature perturbation applied**
 140 **on the (a) left and (b) top boundary of a spatially homogeneous 2D transect at the**
 141 **end of 1-day. (c) The difference in evolved temperature between two cases is many**
 142 **orders of magnitude smaller than the predicted states.**



143

144 **Figure 2 Same as Figure 1 except a sinusoidally varying spatial temperature**
 145 **perturbation is applied.**

146 12) *Where are the locations of center and rim in the model simulations? Fig. 1 shows two*
147 *snow sensors and five temperature sensors. At what locations are the simulation compared to*
148 *the corresponding observations?*

149 **Response:**

150 The dashed line in Figure 2 classifies the 2D transect into rim and center. All grid cells that
151 have surface elevation above the dash line are classified as rim, while all grid cells below
152 the dashed line are marked as center.

153

154 13) *As the authors noted on line 246 that PETSc is a scalable solver, so what is constraining*
155 *the 3D simulation (statement on line 447)?*

156 **Response:**

157 ALM is embarrassing parallel and has no cross processor communication because it is a 1D,
158 vertical-only model. Even though PETSc is a scalable solver, the current implementation of
159 the 3D model is serial. Thus, our model is capable of solving a 3D problem on each
160 processor independently but unable to solve a parallel, 3D problem. We have updated the
161 text in Section 3.5 (Page 19, lines 443-447) to clarify this point.

162

163 14) *Because of the computational constraint, I don't agree with the last statement on line*
164 *510-512.*

165 **Response:**

166 We have updated the text to reflect that the current model is serial (Page 19, Lines 444-
167 445). Even though the current version of the ALM-3D model is sequential, we believe it
168 would be very useful for applications in the Earth System Model context. One potential
169 future application would be to solve 3D subsurface hydrologic and thermal processes
170 within a watershed. To this end, the domain decomposition of ALM in future versions could
171 be modified such that all grid cells within a watershed are assigned to a single processor. In
172 such an application, ALM-3D v1 would be an appropriate candidate.

173

174

175 15) *Figure 1: what's the legend? DEM?*

176 **Response:**

177 The legend indicates the height in meters (now added to Figure 1).

178 **RC2: 'A useful contribution', Anonymous Referee #2**

179

180 General remark. The framework of the paper is Earth System modeling. The authors
181 implement small-scale snow redistribution and 3D soil physics (2D in the setup used here).
182 The results show that a simple snow redistribution parameterization based on
183 microtopography has a very beneficial effect on a range of simulated variables. This is very
184 nice. However, I think that the paper almost entirely misses a thorough discussion of an
185 implementation strategy for these development in the ultimate context of Earth System
186 modeling. This will happen on much larger spatial scales.

187

188 How will you move from an explicit fine-scale representation to a sub grid implementation?
189 Will the choice be only to include snow redistribution (i.e. aren't there already enough
190 results to decide that a 3D soil physics will be an overkill in the Earth System modeling
191 context)? Will the model have two tiles (polygon centers and rims), with snow being
192 shuffled from one tile to the other? Or is the whole thing probably going to be more
193 complex, with an explicit modeling of 3D soil physics supposing an idealized polygon of
194 some finite size? What will be done if the model domain does include areas that are not
195 polygonal tundra (it's supposed to be a global model if I understand correctly)?

196 **Response:**

197 This study is a necessary first step of documenting the role of fine scale processes
198 associated with microtopography and lateral redistribution of water and energy in the
199 subsurface. We acknowledge that a development of a sub grid structure to parsimoniously
200 capture impacts of microtopography and lateral subsurface processes on coarser grid scale
201 is a worthy scientific research, but such a new development is beyond the scope of the
202 current work.

203 However, here are some thoughts on possible approaches to parsimoniously include
204 fine scale processes. As suggested by the reviewer, investigate how accurate is a two-tile
205 approach as compared to explicitly modeling the transect when snow redistribution is
206 accounted for within the model. Additional simulations will be needed to investigate how
207 well the two-tile approach performs when biogeochemical cycling is included. Exclusion of
208 lateral subsurface processes has a greater impact on predicted subgrid variability than on

209 spatially averaged states. Thus, one possible extension of the current model would be to
210 explicitly include an equation for the temporal evolution of sub grid variability of using the
211 approach of Montaldo and Albertson (2003). The use of reduced-order models as described
212 by Pau et al. (2014) is an alternate approach to estimate fine scale hydrologic and thermal
213 states from coarse resolution simulation. We have added discussion of these topics to the
214 Discussion section (page 20, Lines 468-4477)

215

216 If there are issues with computing time already in a 2d setting, is it realistic to go to 3d?

217 **Response:**

218 Moving beyond a 1D land model to a 2D/3D model will certainly increase the
219 computational cost of the simulation. However, the land component is typically the least
220 expensive component of an Earth System Model. ALM is less than 5% of the total
221 computational cost of a fully coupled ACME simulation (ACME Performance team, personal
222 communication, May 25, 2017). Even though there is some leeway in increasing the
223 computational cost of the land model, the need to include higher spatial dimensional
224 processes in land surface models has been made by many studies (Chen et al. (2006); Kim
225 and Mohanty (2016); Maxwell and Condon (2016)). Lateral subsurface processes can be
226 included in the land surface model via a range of numerical discretization approaches of
227 varying complexity such as adding lateral flux of water and energy as source/sink term in
228 the existing 1D model, implementing an operator split approach to solve vertical and
229 lateral processes in a non-iterative model, or solving a fully coupled 3D model. Increased
230 computational cost is not the only factor limiting application of ALM-3D to a global
231 simulation. The subgrid hierarchy structure of the land model, which presently does not
232 have any topological information, needs to be updated to include lateral connectivity. We
233 have added some Discussion on these topics to the revised version (Page 20, Lines 477-
234 483).

235

236 Some words on validation/tests on larger scales?

237 **Response:**

238 Model validation is an integral part of model development. Ongoing projects of the U.S
239 Department of Energy such as the NGEE-Arctic (<https://ngee-arctic.ornl.gov>) and the

240 NGEE-Tropics (<http://ngee-tropics.lbl.gov/>) are expected to provide a wide range datasets
241 related to land surface model at regional scales. Additionally, the Distributed Model
242 Intercomparison Project Phase 2 (DMIP 2) provides a comprehensive datasets and
243 modeling protocol for benchmarking distributed hydrologic models (Smith et al., 2012) and
244 estimates of water table depth at global scales are available from Fan et al. (2013). Our
245 future work will focus on application and validation of ALM-3D at regional scales. We have
246 added some discussion of these issues to the Discussion section (page 20, Lines 483-486)

247

248 Answers to some of these questions might be pretty obvious, but I nevertheless think that a
249 proper discussion of these and other related questions is required.

250 **Response:**

251 We added text in the discussion section that answers all of the questions raised by the
252 reviewer.

253

254 Specific comments.

255 - L.24 : "Three ten-years long simulations" : Is that good English?

256 **Response:**

257 The text has been modified to "Multiple 10-years long simulations"

258

259 - L.55 : "Xu, 2016#154"

260 **Response:**

261 The incorrect citation has now been removed in the updated version of the manuscript.

262

263 - L61: The reference to Friedlingstein et al., 2006 is good but there has been quite some
264 work on this more recently. In general, there are very many pre-2007 references and much
265 less after that period. Maybe the bibliography could be a bit updated. For example, in line
266 78, the review by Schuur et al. in Nature 2015 might be worth citing.

267 **Response:**

268

269 - L.166. "The flow water" -> "The water flow" or "The flow of water"

270 **Response:**

271 The text has been updated to 'The flow of water'.

272

273 - L. 198. I suggest to clarify the writing here. What about this: "... zeta is the diagonal entry
274 of the banded matrix (eq. 11-17)", then provide eq. 11-17. Then: "small phi is a column
275 vector given by:", then put eq. 18. I think that would be clearer.

276 **Response:**

277 As per reviewer suggestions, description of equations 11-18 has been separated into a
278 description of equations 11-17 followed by a description of equation 18.

279

280 - The same applies to eqs. 25-32. Separate eq. 32 from 25-31. I think that eq. 28 should read
281 "eta=..." (not "mu=...") and eq. 29 should read "mu=..." (not "xi=...")

282 **Response:**

283 As per reviewer suggestion, description of equations 25-32 has been separated into two.
284 Additionally, equations 28 and 29 have been correctly updated.

285

286 - Line 232: Please say clearly that this means that there is no geothermal heat flux
287 represented in the model.

288 **Response:**

289 The text updated to explicitly state that geothermal heat flux was not accounted for in this
290 work.

291

292 - L. 261: "to simulate SR", not "to simulated SR"

293 **Response:**

294 The text has been updated.

295

296 - L. 273: "its", not "it's"

297 **Response:**

298 The text has been updated.

299

300 - L.277: A broken link to some internal reference. same at line 328, 342, 343

301 **Response:**

302 All broken references have been updated.

303

304 - L. 285: with do you put the dimension meters in square brackets?

305 **Response:**

306 Square brackets have been removed.

307

308 - L. 289: "SP mode": that's an internal nickname. Its meaning becomes clear at the end of

309 the paper ("satellite phenology") but this is not required here. Either explain the acronym

310 of leave it out.

311 **Response:**

312 Text has been updated to explain the acronym.

313

314

315 **References**

316 Chen, Y., Hall, A., and Liou, K. N.: Application of three-dimensional solar radiative transfer to
317 mountains, *Journal of Geophysical Research: Atmospheres*, 111, n/a-n/a, 2006.

318 Fan, Y., Li, H., and Miguez-Macho, G.: Global Patterns of Groundwater Table Depth, *Science*,
319 339, 940-943, 2013.

320 Kim, J. and Mohanty, B. P.: Influence of lateral subsurface flow and connectivity on soil
321 water storage in land surface modeling, *Journal of Geophysical Research: Atmospheres*,
322 121, 704-721, 2016.

323 Maxwell, R. M. and Condon, L. E.: Connections between groundwater flow and transpiration
324 partitioning, *Science*, 353, 377-380, 2016.

325 Montaldo, N. and Albertson, J. D.: Temporal dynamics of soil moisture variability: 2.
326 Implications for land surface models, *Water Resources Research*, 39, n/a-n/a, 2003.

327 Pau, G. S. H., Bisht, G., and Riley, W. J.: A reduced-order modeling approach to represent
328 subgrid-scale hydrological dynamics for land-surface simulations: application in a
329 polygonal tundra landscape, *Geosci. Model Dev.*, 7, 2091-2105, 2014.

330 Smith, M. B., Koren, V., Reed, S., Zhang, Z., Zhang, Y., Moreda, F., Cui, Z., Mizukami, N.,
331 Anderson, E. A., and Cosgrove, B. A.: The distributed model intercomparison project –
332 Phase 2: Motivation and design of the Oklahoma experiments, *Journal of Hydrology*,
333 418, 3-16, 2012.

334

1 **Impacts of microtopographic snow-redistribution and lateral subsurface processes**
2 **on hydrologic and thermal states in an Arctic polygonal ground ecosystem : A case**
3 **study using ALM-3D v1.0**
4

5 **Gautam Bisht¹, William J. Riley¹, Haruko M. Wainwright¹, Baptiste Dafflon¹, Yuan**
6 **Fengming², and Vladimir E. Romanovsky³**
7

8 ¹Climate & Ecosystem Sciences Division, Lawrence Berkeley National Laboratory,1
9 Cyclotron Road, Berkeley, California 94720, USA
10

11 ²Environmental Sciences Division, Oak Ridge National Laboratory, Oak Ridge, TN, 37831-
12 6301 , USA
13

14 ³Geophysical Institute, University of Alaska Fairbanks, Fairbanks, AK 99775, USA
15

16 Correspondence to: Gautam Bisht (gbisht@lbl.gov)
17

18 **Abstract**

19 Microtopographic features, such as polygonal ground, are characteristic sources of
20 landscape heterogeneity in the Alaskan Arctic coastal plain. Here, we analyze the effects of
21 snow redistribution (SR) and lateral subsurface processes on hydrologic and thermal states
22 at a polygonal tundra site near Barrow, Alaska. We extended the land model integrated in
23 the ACME Earth System Model (ESM) to redistribute incoming snow by accounting for
24 microtopography and incorporated subsurface lateral transport of water and energy (ALM-
25 3D,v1.0). Multiple 10-years long simulations were performed for a transect across
26 polygonal tundra landscape at the Barrow Environmental Observatory in Alaska to isolate
27 the impact of SR and subsurface process representation. When SR was included, model
28 predictions better agreed (higher R^2 , lower bias and RMSE) with observed differences in
29 snow depth between polygonal rims and centers. The model was also able to accurately
30 reproduce observed soil temperature vertical profiles in the polygon rims and centers
31 (overall bias, RMSE, and R^2 of 0.59°C, 1.82°C, and 0.99, respectively). The spatial

Gautam Bisht 8/23/2017 5:29 AM

Deleted: ALMv0

Gautam Bisht 8/23/2017 5:29 AM

Deleted:). Three

Gautam Bisht 8/23/2017 5:29 AM

Deleted: results show a

Gautam Bisht 8/23/2017 5:29 AM

Deleted: agreement

Gautam Bisht 8/23/2017 5:29 AM

Deleted: with

Gautam Bisht 8/23/2017 5:29 AM

Deleted: for the

38 heterogeneity of snow depth during the winter due to SR generated surface soil
39 temperature heterogeneity that propagated in depth and time and led to ~10 cm shallower
40 and ~5 cm deeper maximum annual thaw depths under the polygon rims and centers,
41 respectively. Additionally, SR led to spatial heterogeneity in surface energy fluxes and soil
42 moisture during the summer. Excluding lateral subsurface hydrologic and thermal
43 processes led to small effects on mean states but an overestimation of spatial variability in
44 soil moisture and soil temperature as subsurface liquid pressure and thermal gradients
45 were artificially prevented from spatially dissipating over time. The effect of lateral
46 subsurface processes on maximum thaw depths was modest, with mean absolute
47 differences of ~3 cm. Our integration of three-dimensional subsurface hydrologic and
48 thermal subsurface dynamics in the ACME land model will facilitate a wide range of
49 analyses heretofore impossible in an ESM context.

Gautam Bisht 8/23/2017 5:29 AM
Deleted: active layer
Gautam Bisht 8/23/2017 5:29 AM
Deleted: difference

50 1 Introduction

51 The northern circumpolar permafrost region, which contains ~1700 Pg of organic
52 carbon down to 3 m (Tarnocai et al., 2009), is predicted to experience disproportionately
53 larger future warming compared to the tropics and temperate latitudes (Holland and Bitz,
54 2003). Recent warming in the Arctic has led to changes in lake area (Smith et al., 2005),
55 snow cover duration and extent (Callaghan et al., 2011a), vegetation cover (Sturm et al.,
56 2005), growing season length (Smith et al., 2004), thaw depth (Schuur et al., 2008),
57 permafrost stability (Jorgenson et al., 2006), and land-atmosphere feedbacks (Euskirchen
58 et al., 2009). Future predictions of Arctic warming include northward expansion of shrub
59 cover in tundra (strum 2001, Tape et al 2006), decreases in snow cover duration
60 (Callaghan et al., 2011a), and emissions of CO₂ and CH₄ from decomposition of
61 belowground soil organic matter (Koven et al., 2011; Schaefer et al., 2011; Schuur and
62 Abbott, 2011; Xu et al., 2016).

63 Several recent modeling studies have predicted a positive global carbon-climate
64 feedback at the global scale (Cox et al., 2000; Dufresne et al., 2002; Friedlingstein et al.,
65 2001; Fung et al., 2005; Govindasamy et al., 2011; Jiang et al., 2011; Jones et al., 2003;
66 Koven et al., 2015; Matthews et al., 2007b; Matthews et al., 2005; Sitch et al., 2008;

Gautam Bisht 8/23/2017 5:29 AM
Deleted: ,Xu, 2016 #154
Gautam Bisht 8/23/2017 5:29 AM
Deleted:

71 Thompson et al., 2004; Zeng et al., 2004), although the strength of this predicted feedback
72 at the year 2100 was shown to have a large variability across models (Friedlingstein et al.,
73 2006). In contrast to the ocean carbon cycle, the terrestrial carbon cycle is expected to be a
74 more dominant factor in the global carbon-climate feedback over the next century
75 (Matthews et al., 2007a; Randerson et al., 2015).

76 Snow, which covers the Arctic ecosystem for 8-10 months each year (Callaghan et
77 al., 2011b), is a critical factor influencing hydrologic and ecologic interactions (Jones,
78 1999). Snowpack modifies surface energy balances (via high reflectivity), soil thermal
79 regimes (due to low thermal conductivity), and hydrologic cycles (because of melt water).
80 Several studies have shown that warm soil temperatures under snowpack support the
81 emission of greenhouse gases from belowground respiration (Grogan and Chapin Iii, 1999;
82 Sullivan, 2010) and nitrogen mineralization (Borner et al., 2008; Schimel et al., 2004)
83 during winter. Additionally, decreases in snow cover duration have been shown to increase
84 net ecosystem CO₂ uptake (Galen and Stanton, 1995; Groendahl et al., 2007). Recent snow
85 manipulation experiments in the Arctic have provided evidence of the importance of snow
86 in the expected responses of Arctic ecosystems under future climate change (Morgner et al.,
87 2010; Nobrega and Grogan, 2007; Rogers et al., 2011; Schimel et al., 2004; Wahren et al.,
88 2005; Welker et al., 2000).

89 Apart from the spatial extent and duration of snowpack, the spatial heterogeneity of
90 snow depth is an important factor in various terrestrial processes (Clark et al., 2011;
91 Lundquist and Dettinger, 2005). As synthesized by López-Moreno et al. (2014), the
92 following processes are responsible for snow depth heterogeneity at three distinct spatial
93 scales: microtopography at 1-10 m (Lopez-Moreno et al., 2011); wind induced lateral
94 transport processes at 100-1000 m (Liston et al., 2007); and precipitation variability at
95 catchment scales of 10 – 1000 km (Sexstone and Fassnacht, 2014). The spatial distribution
96 of snow not only affects the quantity of snowmelt discharge (Hartman et al., 1999; Luce et
97 al., 1998), but also the water chemistry (Rohrbough et al., 2003; Wadham et al., 2006;
98 Williams et al., 2001). Lawrence and Swenson (2011) demonstrated the importance of
99 snow depth heterogeneity in predicting responses of the Arctic ecosystem to future climate
100 change by performing idealized numerical simulations of shrub expansion across the pan-
101 Arctic region using the Community Land Model (CLM4). Their results showed that an

Gautam Bisht 8/23/2017 5:29 AM

Deleted: Changes in Arctic ecosystem net ecosystem productivity (NEP, defined as the difference between net primary production (NPP) and heterotrophic respiration (R_h)) will be determined by the magnitude and direction of changes in NPP and R_h. Warming experiments in the Arctic have found increases and decreases of plant growth in response to higher temperatures (Barber et al., 2000; Chapin et al., 1995; Cornelissen et al., 2001; Hobbie and Chapin, 1998; Hollister et al., 2005; Van Wijk et al., 2004; Walker et al., 2006; Wilmling et al., 2004). Arctic ecosystems are limited in nitrogen availability (Schimel et al., 1996; Shaver and Chapin III, 1986) and higher mineralization rates under warmer climate (Hobbie, 1996) could lead to higher CO₂ fixation by plants (Shaver and Chapin, 1991). Additionally, a longer growing season is expected to result in a negative carbon-climate feedback by increasing NPP (Euskirchen et al., 2006). On the other hand, microbial decomposition of previously frozen soil organic matter under a warmer climate is expected to strengthen the carbon-climate feedback (Davidson and Janssens, 2006; Mack et al., 2004; Oechel et al., 1993; Tarnocai et al., 2009).

Gautam Bisht 8/23/2017 5:29 AM

Moved down [1]: The spatial distribution of snow not only affects the quantity of snowmelt discharge (Hartman et al., 1999; Luce et al., 1998), but also the water chemistry (Rohrbough et al., 2003; Wadham et al., 2006; Williams et al., 2001). Lawrence and Swenson (2011) demonstrated the importance of snow depth heterogeneity in predicting responses of the Arctic ecosystem to future climate change by performing idealized numerical simulations of shrub expansion across the pan-Arctic region. [1]

Gautam Bisht 8/23/2017 5:29 AM

Deleted: Their results showed that an increase in active layer thickness (ALT) under shrubs was negated when spatial heterogeneity in snow cover due to wind driven snow redistribution was accounted for, resulting in an unchanged grid cell mean active layer thickness. López-Moreno et al. (2014) identified processes

Gautam Bisht 8/23/2017 5:29 AM

Moved (insertion) [1]

Unknown

Field Code Changed

Unknown

Field Code Changed

169 increase in active layer thickness (ALT), which is the maximum annual thaw depth, under
170 shrubs was negated when spatial heterogeneity in snow cover due to wind driven snow
171 redistribution was accounted for, resulting in an unchanged grid cell mean active layer
172 thickness.

173 Large portions of the Arctic are characterized by polygonal ground features, which
174 are formed in permafrost soil when frozen ground cracks due to thermal contraction
175 during winter and ice wedges form within the upper several meters (Hinkel et al., 2005).
176 Polygons can be classified as 'low-centered' or 'high-centered' based on the relationship
177 between their central and mean elevations. Polygonal ground features are dynamic
178 components of the Arctic landscape in which the upper part of ice-wedge thaw under low-
179 centered polygon troughs leads to subsidence, eventually (~o(centuries)) converting the
180 low-centered polygon into a high-centered polygon (Seppala et al., 1991). Microtopography
181 of polygonal ground influences soil hydrologic and thermal conditions (Engstrom et al.,
182 2005). In addition to controlling CO₂ and CH₄ emissions, soil moisture affects (1)
183 partitioning of incoming radiation into latent, sensible, and ground heat fluxes (Hinzman
184 and Kane, 1992; McFadden et al., 1998); (2) photosynthesis rates (McGuire et al., 2000;
185 Oberbauer et al., 1991; Oechel et al., 1993; Zona et al., 2011); and (3) vegetation
186 distributions (Wiggins, 1951).

187 Our goals in this study include (1) analyzing the effects of spatially heterogeneous
188 snow in polygonal ground on soil temperature and moisture and surface processes (e.g.,
189 surface energy budgets); (2) analyzing how model predictions are affected by inclusion of
190 lateral subsurface hydrologic and thermal processes; and (3) developing and testing a
191 three-dimensional version of the ACME Land Model (ALM; (Tang and Riley, 2016; Zhu and
192 Riley, 2015)), called ALM-3D v1.0 (hereafter ALM-3D). We then applied ALM-3D to a
193 transect across a polygonal tundra landscape at the Barrow Environmental Observatory in
194 Alaska. After defining our study site, the model improvements, model tests against
195 observations, and analyses, we apply the model to examine the effects of snow
196 redistribution and lateral subsurface processes on snow micro-topographical
197 heterogeneity, soil temperature, and the surface energy budget.

Gautam Bisht 8/23/2017 5:29 AM

Deleted: land model

Gautam Bisht 8/23/2017 5:29 AM

Deleted: integrated in the ACME Earth System Model (ESM). We note that the original version of ALM is equivalent to CLM4.5 (Koven et al., 2013; Oleson, 2013a), and represents vertical energy and water dynamics, including phase change. We expanded on that model to explicitly represent soil lateral energy and hydrological exchanges and fine-resolution snow redistribution (ALMv0-3D). We then applied ALMv0

210 2 Methodology

211 2.1 Study Area

212 Our analysis focuses on sites located near Barrow, Alaska (71.3° N, 156.5° W) from
213 the long term Department of Energy (DOE) Next-Generation Ecosystem Experiment (NGEE-
214 Arctic) project. The four primary NGEE-Arctic study sites (A, B, C, D) are located within the
215 Barrow Environmental Observatory (BEO), which is situated on the Alaskan Coastal Plain.
216 The annual mean air temperature for our study sites is approximately -13°C (Walker et al.,
217 2005) and mean annual precipitation is 106 mm with the majority of precipitation
218 occurring during the summer season (Wu et al., 2013). The study site is underlain with
219 continuous permafrost (Brown et al., 1980) and the annual maximum thaw depth (active
220 layer depth) ranges between 30-90 cm (Hinkel et al., 2003). Although the overall
221 topographic relief for the BEO is low, the four NGEE study sites have distinct
222 microtopographic features: low-centered (A), high-centered (B), and transitional polygons
223 (C, D). Contrasting polygon types are indicative of different stages of permafrost
224 degradation and were the primary motivation behind the choice of study sites for the
225 NGEE-Arctic project. LIDAR Digital Elevation Model (DEM) data were available at 0.25 m
226 resolution for the region encompassing all four NGEE sites. In this work, we perform
227 simulations along a two-dimensional transect in low-centered polygon Site-A as shown by
228 the dotted line in Figure 1.

229 2.2 ALMv0 Description

230 The original version of ALM is equivalent to CLM4.5 (Koven et al., 2013; Oleson,
231 2013b; Ghimire et al., 2016), and represents vertical energy and water dynamics, including
232 phase change. We developed ALM-3D by expanding on that model to explicitly represent
233 soil lateral energy and hydrological exchanges and fine-resolution snow redistribution. We
234 run ALM-3D here with prescribed plant phenology (called Satellite Phenology (SP) mode),
235 since our focus is on thermal dynamics of the system, rather than C cycle dynamics.

Gautam Bisht 8/23/2017 5:29 AM

Deleted: We developed the capability to represent three-dimensional hydrology and thermal dynamics in ALMv0 (Zhu et al., 2016b), and call the new model ALMv0-3D. ALMv0 was derived from CLM4.5 (Ghimire et al., 2016; Koven et al., 2013), and is the land model integrated in the ACME Earth System Model (ESM). The model represents coupled plant biophysics, soil hydrology, and soil biogeochemistry (Oleson *et al.* 2013). We run ALMv0-3D here with prescribed plant phenology (called Satellite Phenology (SP) mode), since our focus is on the thermal dynamics of the system, rather than the C cycle dynamics. .

251 2.3 Representing Two- and Three-Dimensional Physics

252 2.3.1 Subsurface hydrology

253 The flow of water in the unsaturated zone is given by the θ -based Richards
254 equations as

$$\frac{\partial \theta}{\partial t} = -\nabla \cdot \vec{q} - Q \quad (1)$$

255 where θ [m^3m^{-3}] is the volumetric soil water content, t [s] is time, \vec{q} [ms^{-1}] is Darcy flux, and
256 Q [m^3 of water m^{-3} of soil s^{-1}] is volumetric sink of water. Darcy flux is given by

$$\vec{q} = -k\nabla(\psi + z) \quad (2)$$

257 where k [ms^{-1}] is the hydraulic conductivity, ψ [m] is the soil matric potential, and z [m] is
258 height above a reference datum. The hydraulic conductivity and soil matric potential are
259 non-linear functions of volumetric soil moisture. ALMv0 uses the modified form of Richards
260 equation of Zeng and Decker (2009) that computes Darcy flux as

$$\vec{q} = -k\nabla(\psi + z - C) \quad (3)$$

261 where C is a constant hydraulic potential above the water table, z_v , given as

$$C = \psi_E + z = \psi_{sat} \left[\frac{\theta_E(z)}{\theta_{sat}} \right]^{-B} + z = \psi_{sat} + z_v \quad (4)$$

262 where ψ_E [m] is the equilibrium soil matric potential, ψ_{sat} [m] is the saturated soil matric
263 potential, θ_E [m^3m^{-3}] is volumetric soil water content at equilibrium soil matric potential,
264 θ_{sat} [m^3m^{-3}] is volumetric soil water content at saturation, z_v [m] is height of water table
265 above the reference datum, and B [-] is a fitting parameter for soil-water characteristic
266 curves. Substituting equations (3) and (4) into equation (1) yields the equation for the
267 vertical transport of water in ALMv0:

$$\frac{\partial \theta}{\partial t} = \frac{\partial}{\partial z} \left[k \left(\frac{\partial(\psi - \psi_E)}{\partial z} \right) \right] - Q \quad (5)$$

268 A finite volume spatial discretization and implicit temporal discretization with Taylor
269 series expansion leads to a tri-diagonal system of equations. We extended this 1-D Richards
270 equation to a 3-D representation integrated in ALM-3D, which is presented next.

271 We use a cell-centered finite volume discretization to decompose the spatial domain
272 into N non-overlapping control volumes, Ω_n , such that $\Omega = \bigcup_{n=1}^N \Omega_n$ and Γ_n represents the

Gautam Bisht 8/23/2017 5:29 AM

Deleted: and

Gautam Bisht 8/23/2017 5:29 AM

Deleted: .

Gautam Bisht 8/23/2017 5:29 AM

Deleted: ALMv0

276 boundary of the n -th control volume. Applying a finite volume integral to equation (1) and
 277 the divergence theorem yields

$$\frac{\partial}{\partial t} \int_{\Omega_n} \theta dV = - \int_{\Gamma_n} (\vec{q} \cdot d\vec{A}) - \int_{\Omega_n} Q dV \quad (6)$$

278 The spatially discretized equation for the n -th grid cell that has V_n volume and n' neighbors
 279 is given by

$$\frac{d\theta_n}{dt} V_n = - \sum_{n'} (\vec{q}_{nn'} \cdot \vec{A}_{nn'}) - QV_n \quad (7)$$

280 For the sake of simplicity in presenting the discretized equation, we assume the 3-D grid is
 281 a Cartesian grid with each grid cell having a thickness of Δx , Δy , and Δz in the x , y , and z
 282 directions, respectively. Using an implicit time integral, the 3-D discretized equation at time
 283 $t + 1$ for a (i, j, k) control volume is given as

$$\begin{aligned} \left(\frac{\Delta\theta_{i,j,k}^{t+1}}{\Delta t} \right) V_{i,j,k} &= (q_{x_{i-1/2,j,k}}^{t+1} - q_{x_{i+1/2,j,k}}^{t+1}) \Delta y \Delta z \\ &+ (q_{y_{i,j-1/2,k}}^{t+1} - q_{y_{i,j+1/2,k}}^{t+1}) \Delta x \Delta z \\ &+ (q_{z_{i,j,k-1/2}}^{t+1} - q_{z_{i,j,k+1/2}}^{t+1}) \Delta x \Delta y - QV_{i,j,k} \end{aligned} \quad (8)$$

284 where q_x , q_y and q_z are Darcy flux in the x , y , and z directions, respectively and $\Delta\theta_{i,j,k}^{t+1}$ is the
 285 change in volumetric soil liquid water in time Δt . [Using the same approach as Oleson](#)
 286 [\(2013a\)](#), the Darcy flux in all three directions is linearized about θ using Taylor series
 287 expansion. The linearized Darcy flux in the x direction at the $(i - 1/2, j, k)$ interface is a
 288 function of $\theta_{i-1,j,k}$ and $\theta_{i,j,k}$:

$$q_{x_{i-1/2,j,k}}^{t+1} = q_{x_{i-1/2,j,k}}^t + \frac{\partial q_{x_{i-1/2,j,k}}^t}{\partial \theta_{i-1,j,k}} \Delta\theta_{i-1,j,k}^{t+1} + \frac{\partial q_{x_{i-1/2,j,k}}^t}{\partial \theta_{i,j,k}} \Delta\theta_{i,j,k}^{t+1} \quad (9)$$

289 The linearized Darcy fluxes in the y and z directions are computed similarly. Substituting
 290 equation (9) in equation (8) results in a banded matrix of the form

$$\begin{aligned} \alpha \Delta\theta_{i-1,j,k}^{t+1} + \beta \Delta\theta_{i,j-1,k}^{t+1} + \gamma \Delta\theta_{i,j,k-1}^{t+1} + \eta \Delta\theta_{i+1,j,k}^{t+1} + \mu \Delta\theta_{i,j+1,k}^{t+1} + \phi \Delta\theta_{i,j,k+1}^{t+1} \\ + \zeta \Delta\theta_{i,j,k}^{t+1} = \varphi \end{aligned} \quad (10)$$

291 where α , β , and γ are subdiagonal entries; η , μ , and ϕ are superdiagonal entries; ζ is
 292 diagonal entry of the banded matrix, [is](#) given by

Gautam Bisht 8/23/2017 5:29 AM

Deleted: Using the same approach as Oleson (2013b)

Gautam Bisht 8/23/2017 5:29 AM

Deleted: ; and φ is a column vector

	$\alpha = \frac{\partial q_{x_{i-1/2,j,k}}^t}{\partial \theta_{i-1,j,k}} \Delta y \Delta z$	(11)
	$\beta = \frac{\partial q_{y_{i,j-1/2,k}}^t}{\partial \theta_{i,j-1,k}} \Delta x \Delta z$	(12)
	$\gamma = \frac{\partial q_{z_{i,j,k-1/2}}^t}{\partial \theta_{i,j,k-1}} \Delta x \Delta y$	(13)
	$\eta = \frac{\partial q_{x_{i+1/2,j,k}}^t}{\partial \theta_{i+1,j,k}} \Delta y \Delta z$	(14)
	$\mu = \frac{\partial q_{y_{i,j+1/2,k}}^t}{\partial \theta_{i,j+1,k}} \Delta x \Delta z$	(15)
	$\phi = \frac{\partial q_{z_{i,j,k+1/2}}^t}{\partial \theta_{i,j,k+1}} \Delta x \Delta y$	(16)
	$\zeta = \left(\frac{\partial q_{x_{i-1/2,j,k}}^t}{\partial \theta_{i,j,k}} - \frac{\partial q_{x_{i+1/2,j,k}}^t}{\partial \theta_{i,j,k}} \right) \Delta y \Delta z + \left(\frac{\partial q_{y_{i,j-1/2,k}}^t}{\partial \theta_{i,j,k}} - \frac{\partial q_{y_{i,j+1/2,k}}^t}{\partial \theta_{i,j,k}} \right) \Delta x \Delta z$ $+ \left(\frac{\partial q_{z_{i,j,k-1/2}}^t}{\partial \theta_{i,j,k}} - \frac{\partial q_{z_{i,j,k+1/2}}^t}{\partial \theta_{i,j,k}} \right) \Delta x \Delta y - \frac{\Delta x \Delta x \Delta z}{\Delta t}$	(17)

Gautam Bisht 8/23/2017 5:29 AM
Formatted Table

Gautam Bisht 8/23/2017 5:29 AM
Deleted: $\left(\frac{\partial q_{z_{i,j-1/2,k}}^t}{\partial \theta_{i,j,k}} - \frac{\partial q_{z_{i,j+1/2,k}}^t}{\partial \theta_{i,j,k}} \right)$

Gautam Bisht 8/23/2017 5:29 AM
Deleted: $\varphi = - \left(q_{x_{i-1/2,j,k}}^t - q_{x_{i+1/2,j,k}}^t \right) \Delta y \Delta z - \left(q_{y_{i,j-1/2,k}}^t - q_{y_{i,j+1/2,k}}^t \right) \Delta x \Delta z - \left(q_{z_{i,j-1/2,k}}^t - q_{z_{i,j+1/2,k}}^t \right) \Delta x \Delta y + Q_{i,j,k}^{t+1} \Delta x \Delta x \Delta z$... [2]

296

297 The column vector φ is given by

$$\varphi = - \left(q_{x_{i-1/2,j,k}}^t - q_{x_{i+1/2,j,k}}^t \right) \Delta y \Delta z - \left(q_{y_{i,j-1/2,k}}^t - q_{y_{i,j+1/2,k}}^t \right) \Delta x \Delta z$$

$$- \left(q_{z_{i,j,k-1/2}}^t - q_{z_{i,j,k+1/2}}^t \right) \Delta x \Delta y + Q_{i,j,k}^{t+1} \Delta x \Delta x \Delta z \quad (18)$$

298

299 The coefficients of equation (10) described in equation (11)-(18) are for an internal grid
300 cell with six neighbors. The coefficients for the top and bottom grid cells are modified for
301 infiltration and interaction with the unconfined aquifer in the same manner as [Oleson](#)
302 [\(2013a\)](#). Similarly, the coefficients for the grid cells on the lateral boundary are modified
303 for a no-flux boundary condition. [See Oleson \(2013a\)](#) for details about the computation of
304 hydraulic properties and derivative of Darcy flux with respect to soil liquid water content.

Gautam Bisht 8/23/2017 5:29 AM
Deleted: Oleson (2013b).

Gautam Bisht 8/23/2017 5:29 AM
Deleted: See Oleson (2013b)

312 2.3.2 Subsurface thermal

313 ALMv0 solves a tightly coupled system of equations for soil, snow, and standing
314 water temperature (Oleson, 2013b). The model solves the transient conservation of
315 energy:

$$c \frac{\partial T}{\partial t} = -\nabla \cdot \mathbf{F} \quad (19)$$

316 where c is the volumetric heat capacity [$\text{J m}^{-3} \text{K}^{-1}$], \mathbf{F} is the heat flux [W m^{-2}], and t is time
317 [s]. The heat conduction flux is given by

$$\mathbf{F} = -\lambda \nabla T \quad (20)$$

318 where λ is thermal conductivity [$\text{W m}^{-1} \text{K}^{-1}$] and T is temperature [K]. Applying a finite
319 volume integral to equation (20) and divergence theorem yields

$$c \frac{\partial}{\partial t} \int_{\Omega_n} T = - \int_{\Gamma_n} \vec{\mathbf{F}} \cdot d\vec{\mathbf{A}} \quad (21)$$

320 The spatially discretized equation for a n -th grid cell that has V_n volume and n' neighbors is
321 given by

$$c_n \frac{dT_n}{dt} V_n = - \sum_{n'} (\vec{\mathbf{F}}_{nn'} \cdot \vec{\mathbf{A}}_{nn'}) \quad (22)$$

322 Similar to the approach taken in Section 2.3.1, ALM-3D assumes a 3-D Cartesian grid with
323 each grid cell having a thickness of Δx , Δy , and Δz in the x , y , and z directions, respectively.
324 Temporal integration of equation (22) is carried out using the Crank-Nicholson method
325 that uses a linear combination of fluxes evaluated at time t and $t + 1$:

Gautam Bisht 8/23/2017 5:29 AM

Deleted: (Oleson, 2013a).

Gautam Bisht 8/23/2017 5:29 AM

Deleted: ALMv0

$$\begin{aligned}
& \frac{c_{n_{i,j,k}}}{\Delta t} (T_{i,j,k}^{t+1} - T_{i,j,k}^t) \Delta x \Delta y \Delta z \\
&= \omega \left\{ \left(F_{x_{i-1/2,j,k}}^t - F_{x_{i+1/2,j,k}}^t \right) \Delta y \Delta z + \left(F_{y_{i,j-1/2,k}}^t - F_{y_{i,j+1/2,k}}^t \right) \Delta x \Delta z \right. \\
&+ \left. \left(F_{z_{i,j,k-1/2}}^t - F_{z_{i,j,k+1/2}}^t \right) \Delta x \Delta y \right\} \\
&+ (1 - \omega) \left\{ \left(F_{x_{i-1/2,j,k}}^{t+1} - F_{x_{i+1/2,j,k}}^{t+1} \right) \Delta y \Delta z \right. \\
&+ \left. \left(F_{y_{i,j-1/2,k}}^{t+1} - F_{y_{i,j+1/2,k}}^{t+1} \right) \Delta x \Delta z \right. \\
&+ \left. \left(F_{z_{i,j,k-1/2}}^{t+1} - F_{z_{i,j,k+1/2}}^t + 1 \right) \Delta x \Delta y \right\} \quad (23)
\end{aligned}$$

328 where ω is the weight in the Crank-Nicholson method and set to 0.5 in this study.

329 Substituting a discretized form of heat flux using equation (20) in equation (23), results in
330 a banded matrix of the form

$$\begin{aligned}
& \alpha T_{i-1,j,k}^{t+1} + \beta T_{i,j-1,k}^{t+1} + \gamma T_{i,j,k-1}^{t+1} + \eta T_{i+1,j,k}^{t+1} + \mu T_{i,j+1,k}^{t+1} + \phi T_{i,j,k+1}^{t+1} + \zeta \Delta T_{i,j,k}^{t+1} \\
&= \varphi \quad (24)
\end{aligned}$$

331 where $\alpha, \beta,$ and γ are subdiagonal entries; $\eta, \mu,$ and ϕ are superdiagonal entries; ζ is
332 diagonal entry of the banded matrix is given by

$$\alpha = \left(\frac{-(1 - \omega) \Delta t}{c_{n_{i,j,k}} \Delta x} \right) \left(\frac{\lambda_{i-1/2,j,k}}{x_{i,j,k} - x_{i-1,j,k}} \right) \quad (25)$$

333

$$\beta = \left(\frac{-(1 - \omega) \Delta t}{c_{n_{i,j,k}} \Delta y} \right) \left(\frac{\lambda_{i,j-1/2,k}}{y_{i,j,k} - y_{i-1,j,k}} \right) \quad (26)$$

334

$$\gamma = \left(\frac{-(1 - \omega) \Delta t}{c_{n_{i,j,k}} \Delta z} \right) \left(\frac{\lambda_{i,j,k-1/2}}{z_{i,j,k} - z_{i,j,k-1}} \right) \quad (27)$$

335

$$\eta = \left(\frac{-(1 - \omega) \Delta t}{c_{n_{i,j,k}} \Delta x} \right) \left(\frac{\lambda_{i+1/2,j,k}}{x_{i+1,j,k} - x_{i,j,k}} \right) \quad (28)$$

336

Gautam Bisht 8/23/2017 5:29 AM

Deleted: $c_n \frac{(T_{i,j,k}^{t+1} - T_{i,j,k}^t)}{\Delta t} \Delta x \Delta y \Delta z =$
 $\omega \left\{ \left(F_{x_{i-1/2,j,k}}^t - F_{x_{i+1/2,j,k}}^t \right) \Delta y \Delta z + \left(F_{y_{i,j-1/2,k}}^t - F_{y_{i,j+1/2,k}}^t \right) \Delta x \Delta z + \left(F_{z_{i,j,k-1/2}}^t - F_{z_{i,j,k+1/2}}^t \right) \Delta x \Delta y \right\} + (1 - \omega) \left\{ \left(F_{x_{i-1/2,j,k}}^{t+1} - F_{x_{i+1/2,j,k}}^{t+1} \right) \Delta y \Delta z + \left(F_{y_{i,j-1/2,k}}^{t+1} - F_{y_{i,j+1/2,k}}^{t+1} \right) \Delta x \Delta z + \left(F_{z_{i,j,k-1/2}}^{t+1} - F_{z_{i,j,k+1/2}}^t + 1 \right) \Delta x \Delta y \right\}$

Gautam Bisht 8/23/2017 5:29 AM

Deleted: ; and φ is a column vector

Gautam Bisht 8/23/2017 5:29 AM

Deleted: $\left(\frac{-\omega' \Delta t}{c_{i,j,k} \Delta x} \right)$

Gautam Bisht 8/23/2017 5:29 AM

Deleted: $\left(\frac{-\omega' \Delta t}{c_{i,j,k} \Delta y} \right)$

Gautam Bisht 8/23/2017 5:29 AM

Deleted: $\left(\frac{-\omega' \Delta t}{c_{i,j,k} \Delta z} \right)$

Gautam Bisht 8/23/2017 5:29 AM

Deleted: $\mu = \left(\frac{-\omega' \Delta t}{c_{i,j,k} \Delta x} \right)$

$$\mu = \left(\frac{-(1-\omega)\Delta t}{c_{n_{i,j,k}}\Delta y} \right) \left(\frac{\lambda_{i-1/2,j,k}}{y_{i+1,j,k} - y_{i,j,k}} \right) \quad (29)$$

Gautam Bisht 8/23/2017 5:29 AM

Deleted: $\xi = \left(\frac{-\omega'\Delta t}{c_{i,j,k}\Delta y} \right)$

$$\phi = \left(\frac{-(1-\omega)\Delta t}{c_{n_{i,j,k}}\Delta z} \right) \left(\frac{\lambda_{i-1/2,j,k}}{z_{i+1,j,k} - z_{i,j,k}} \right) \quad (30)$$

Gautam Bisht 8/23/2017 5:29 AM

Deleted: $\left(\frac{-\omega'\Delta t}{c_{i,j,k}\Delta z} \right)$

$$\begin{aligned} \zeta = 1 + & \left(\frac{(1-\omega)\Delta t}{c_{n_{i,j,k}}\Delta x} \right) \left[\frac{\lambda_{i-1/2,j,k}}{x_{i,j,k} - x_{i-1,j,k}} + \frac{\lambda_{i+1/2,j,k}}{x_{i+1,j,k} - x_{i,j,k}} \right] \\ & + \left(\frac{(1-\omega)\Delta t}{c_{n_{i,j,k}}\Delta y} \right) \left[\frac{\lambda_{i,j-1/2,k}}{y_{i,j,k} - y_{i,j,k-1}} + \frac{\lambda_{i,j+1/2,k}}{y_{i+1,j,k} - y_{i,j,k}} \right] \\ & + \left(\frac{(1-\omega)\Delta t}{c_{n_{i,j,k}}\Delta z} \right) \left[\frac{\lambda_{i,j,k-1/2}}{z_{i,j,k} - z_{i,j,k-1}} + \frac{\lambda_{i,j,k+1/2}}{z_{i+1,j,k} - z_{i,j,k}} \right] \end{aligned} \quad (31)$$

Gautam Bisht 8/23/2017 5:29 AM

Deleted: $\zeta = 1 + \left(\frac{\omega'\Delta t}{c_{i,j,k}\Delta x} \right) \left[\frac{\lambda_{i-1/2,j,k}}{x_{i,j,k} - x_{i-1,j,k}} + \frac{\lambda_{i+1/2,j,k}}{x_{i+1,j,k} - x_{i,j,k}} \right] + \left(\frac{\omega'\Delta t}{c_{i,j,k}\Delta y} \right) \left[\frac{\lambda_{i,j-1/2,k}}{y_{i,j,k} - y_{i,j,k-1}} + \frac{\lambda_{i,j+1/2,k}}{y_{i+1,j,k} - y_{i,j,k}} \right] + \left(\frac{\omega'\Delta t}{c_{i,j,k}\Delta z} \right) \left[\frac{\lambda_{i,j,k-1/2}}{z_{i,j,k} - z_{i,j,k-1}} + \frac{\lambda_{i,j,k+1/2}}{z_{i+1,j,k} - z_{i,j,k}} \right]$

The column vector ϕ is given by

$$\begin{aligned} \phi = T_{i,j,k}^t + & \left(\frac{\omega\Delta t}{c_{n_{i,j,k}}\Delta x} \right) (F_{x_{i-1/2,j,k}}^t - F_{x_{i+1/2,j,k}}^t) \\ & + \left(\frac{\omega\Delta t}{c_{n_{i,j,k}}\Delta y} \right) (F_{y_{i,j-1/2,k}}^t - F_{y_{i,j+1/2,k}}^t) \\ & + \left(\frac{\omega\Delta t}{c_{n_{i,j,k}}\Delta z} \right) (F_{z_{i,j,k-1/2}}^t - F_{z_{i,j,k+1/2}}^t) \end{aligned} \quad (32)$$

Gautam Bisht 8/23/2017 5:29 AM

Deleted: $\left(\frac{\omega\Delta t}{c_{i,j,k}\Delta x} \right)$

Gautam Bisht 8/23/2017 5:29 AM

Deleted: $\left(\frac{\omega\Delta t}{c_{i,j,k}\Delta y} \right)$

Gautam Bisht 8/23/2017 5:29 AM

Deleted: $\left(\frac{\omega\Delta t}{c_{i,j,k}\Delta z} \right) (F_{z_{i,j,k-1/2}}^t - F_{z_{i,j,k+1/2}}^t)$

The coefficients of equation (24) described in equation (25)-(32) are for an internal grid cell with six neighbors. The coefficients for the top grid cells are modified for presence of snow and/or standing water. A no-flux boundary condition was applied on the bottom grid cells, thus no geothermal flux was accounted for in this study. The coefficients for the grid cells on the lateral boundary are modified for a no-flux boundary condition. ALM handles ice-liquid phase transitions by first predicting temperatures at the end of a time step and then updating temperatures after accounting for deficits or excesses of energy during melting or freezing. See Oleson (2013a) for details about the computation of thermal properties and phase transition.

Gautam Bisht 8/23/2017 5:29 AM

Deleted: 32

Gautam Bisht 8/23/2017 5:29 AM

Deleted: and bottom

Gautam Bisht 8/23/2017 5:29 AM

Deleted: , and

Unknown

Field Code Changed

Gautam Bisht 8/23/2017 5:29 AM

Deleted: 2013b

377 **2.3.3 PETSc Numerical solution**
378 ALMv0, which considers flow only in the vertical direction, solves a tridiagonal and
379 banded tridiagonal system of equations for water and energy transport, respectively. In
380 ALM-3D, accounting for lateral flow in the subsurface results in a sparse linear system,
381 equations (10) and (24), where the sparsity pattern of the linear system depends on grid
382 cell connectivity. In this work, we use the PETSc (Portable, Extensible Toolkit for Scientific
383 Computing) library (Balay et al., 2016) developed at the Argonne National Laboratory to
384 solve the sparse linear systems. PETSc provides object-oriented data structures and solvers
385 for scalable scientific computation on parallel supercomputers. [Description about the](#)
386 [numerical tests that were conducted to ensure the lateral coupling of hydrologic and](#)
387 [thermal processes was correctly implemented is presented in supplementary material](#)
388 [\(Figure S 1 and S 2\)](#)

Gautam Bisht 8/23/2017 5:29 AM
Deleted: via PETSc

Gautam Bisht 8/23/2017 5:29 AM
Deleted: ALMv0

389 2.4 Snow Model and Redistribution

390 The snow model in ALM-3D is the same as that in the default ALMv0 and CLM4.5
391 (Anderson, 1976; Dai and Zeng, 1997; Jordan, 1991), [except for the inclusion of snow](#)
392 [redistribution \(SR\)](#). The snow model allows for a dynamic snow depth and up to [five](#) snow
393 layers, and explicitly solves the vertically-resolved mass and energy budgets. Snow aging,
394 compaction, and phase change are all represented in the snow model formulation.
395 Additionally, the snow model accounts for the influence of aerosols (including black and
396 organic carbon and mineral dust) on snow radiative transfer ([Oleson, 2013b](#)). ALMv0 uses
397 the methodology of Swenson and Lawrence (2012) to compute fractional snow cover area,
398 which is appropriate for ESM-scale grid cells (~100 km x 100 km). Since the grid cell
399 resolution in this work is sub-meter, we modified the fractional cover to be either 1 (when
400 snow was present) or 0 (when snow was absent).

Gautam Bisht 8/23/2017 5:29 AM
Deleted: ALMv0

Gautam Bisht 8/23/2017 5:29 AM
Deleted: .

Gautam Bisht 8/23/2017 5:29 AM
Deleted: 5

401 Two main drivers of SR include topography and surface wind (Warscher et al.,
402 2013); previous SR models include mechanistically- (Bartelt and Lehning, 2002; Liston and
403 Elder, 2006) and empirically- (Frey and Holzmann, 2015; Helfricht et al., 2012) based
404 approaches. To mimic the effects of wind, we used a conceptual model to [simulate](#) SR over
405 the fine-resolution topography of our site by instantaneously re-distributing the incoming
406 snow flux such that lower elevation areas (polygon center) receive snow before higher

Gautam Bisht 8/23/2017 5:29 AM
Deleted: (Oleson, 2013a). ALMv0

Gautam Bisht 8/23/2017 5:29 AM
Deleted: [

Gautam Bisht 8/23/2017 5:29 AM
Deleted:]

Gautam Bisht 8/23/2017 5:29 AM
Deleted: [

Gautam Bisht 8/23/2017 5:29 AM
Deleted:]).

Gautam Bisht 8/23/2017 5:29 AM
Deleted: snow redistribution (

Gautam Bisht 8/23/2017 5:29 AM
Deleted:)

Gautam Bisht 8/23/2017 5:29 AM
Deleted: simulated

420 elevation areas (polygon rims). This relatively simple and parsimonious approach is
421 reasonable given the observed snow depth heterogeneity, as described below, and small
422 spatial extent of our domain.

423 2.5 System Characterization

424 Hydrologic and thermal properties differ by depth and landscape type. We used the
425 horizontal distribution of organic matter (OM) content from Wainwright et al. (2015) to
426 infer soil hydrologic and thermal properties following the default representations in ALM.
427 Vegetation cover was classified as arctic shrubs in polygon centers and arctic grasses in
428 polygon rims. The default representation of the plant wilting factor assigns a value of zero
429 for a given soil layer when its temperature falls below a threshold ($T_{\text{threshold}}$) of -2°C . This
430 default value leads to overly large predicted latent and sensible heat fluxes during winter,
431 compared to nearby eddy covariance measurements. We modified $T_{\text{threshold}}$ to be 0°C in this
432 study, resulting in improved predicted wintertime latent heat fluxes compared to the
433 default version of the model (Figure S3). Although biases compared to the observations
434 remain, particularly for sensible heat fluxes in the spring, the improvement is substantial
435 and, given the observational uncertainties, we believe sufficient to justify our use of the
436 model for investigations of the role of snow heterogeneity in this polygonal tundra system.

437 2.6 Simulation Setup, Climate Forcing, and Analyses

438 Because of computational constraints, we investigated the role of snow
439 redistribution and physics representation using a two-dimensional transect through site A
440 (Figure 1). The transect was 104 m long and 45 m deep and was discretized horizontally
441 with a grid spacing of 0.25 m and an exponentially varying layer thickness in the vertical
442 with 30 soil layers. No flow conditions for mass and energy were imposed on the east, west,
443 and bottom boundaries of the domain. Temporal discretization of 30 min was used in the
444 simulations. All simulations were performed in the “satellite phenology” (SP) mode, i.e.,
445 Leaf Area Index (LAI) was prescribed from MODIS observations.

446 Simulations were run for 10 years using long-term climate data gathered at the
447 Barrow, Alaska Observatory site (<https://www.esrl.noaa.gov/gmd/obop/brw/>) managed
448 by the Global Monitoring Division of NOAA’s Earth System Research Laboratory (Mefford et

Gautam Bisht 8/23/2017 5:29 AM
Deleted: OM

Gautam Bisht 8/23/2017 5:29 AM
Deleted: it's

Gautam Bisht 8/23/2017 5:29 AM
Deleted: (Error! Reference source not found.)

Gautam Bisht 8/23/2017 5:29 AM
Deleted: [

Gautam Bisht 8/23/2017 5:29 AM
Deleted:]

Gautam Bisht 8/23/2017 5:29 AM
Deleted: [

Gautam Bisht 8/23/2017 5:29 AM
Deleted:]

Gautam Bisht 8/23/2017 5:29 AM
Deleted: that

Gautam Bisht 8/23/2017 5:29 AM
Deleted: [

Gautam Bisht 8/23/2017 5:29 AM
Deleted:]

Gautam Bisht 8/23/2017 5:29 AM
Deleted: [

Gautam Bisht 8/23/2017 5:29 AM
Deleted:]

Gautam Bisht 8/23/2017 5:29 AM
Deleted: “

Gautam Bisht 8/23/2017 5:29 AM
Deleted: ”

464 al., 1996). The missing precipitation time series was gap-filled using daily precipitation at
465 the Barrow Regional Airport available from the Global Historical Climatology Network
466 (<http://www1.ncdc.noaa.gov/pub/data/ghcn/daily>). We tested the model by comparing
467 predictions to high-frequency observations of snow depth and vertically resolved soil
468 temperature for September 2012 – September 2013. Temperature observations were
469 taken at discrete locations in a polygon center and rim (Figure 1), and were combined to
470 analyze comparable landscape positions in the simulations (Figure 2).

471 After testing, the model was used to investigate the effects of snow redistribution
472 and 2D subsurface hydrologic and thermal physics by analyzing three scenarios: (1) no
473 snow redistribution and 1D physics; (2) snow redistribution and 1D physics; and (3) snow
474 redistribution and 2D physics. Between these scenarios, we compared vertically-resolved
475 soil temperature and liquid saturation, active layer depth, and mean and spatial variation of
476 latent and sensible heat fluxes across the 10 years of simulations. For each soil column, the
477 simulated soil temperature was interpolated vertically and the active layer depth was
478 estimated as the maximum depth that had above-freezing soil temperature.

479 3 Results and Discussion

480 3.1 Snow depth

481 In the absence of SR, predicted snow depth exactly follows the topography. With SR,
482 a much smaller dependence of winter-average snow depth on topography is predicted
483 (Figure 2). Further, for the winter average, there are very small differences in snow depth
484 between simulations with SR and 1D or 2D subsurface physics representations. Compared
485 to observations, considering SR led to: (1) a factor of ~2 improvement in snow depth bias
486 for the polygon center; (2) modest increase and decrease in average bias on the rims for
487 September through February and March through June, respectively; and (3) a dramatic
488 improvement in bias of the difference in snow depth between the polygon centers and rims
489 (Figure 3). There was no discernible difference in snow depth bias between the 1D and 2D
490 physics (Table 1), although the predicted subsurface temperature fields were different, as
491 shown below.

Gautam Bisht 8/23/2017 5:29 AM

Deleted: effect

Gautam Bisht 8/23/2017 5:29 AM

Deleted: larger

Gautam Bisht 8/23/2017 5:29 AM

Deleted: snow redistribution

495 The temporal variation of the mean snow depth (**Figure 4a**) and its spatial standard
496 deviation (**Figure 4b**) also differed based on whether SR was considered, but was not
497 affected by considering 2D thermal or hydrologic physics. With SR, the snow depth
498 coefficient of variation (**Figure 4c**) was about 0.5 from December through the beginning of
499 the snowmelt period, indicating relatively large spatial heterogeneity. Simulated snow
500 depth for the three simulation scenarios are included in Supplementary Material (4)

Gautam Bisht 8/23/2017 5:29 AM
Deleted: Snapshots of simulated

501 3.2 Soil Temperature and Active Layer Depth

502 Broadly, ALM-3D accurately predicted the polygon center soil temperature at depth
503 intervals corresponding to the temperature probes (0-20 cm, 20-50 cm, 50-75 cm, and 75-
504 100 cm; Figure 5a). Recall that the observed temperatures for the polygon center and rims
505 were taken at single points in site A (Figure 1) while the predicted temperatures were
506 calculated as averages across the transect for each of the two landscape position types. The
507 model was able to simulate early freeze up of the soil column under the rims as compared
508 to centers in November 2012 because of differences in accumulated snow pack. The
509 transition to thawed soil in the 0-20 cm depth interval in early June 2013 and the
510 subsequent temperature dynamics over the summer were very well captured by ALM-3D.
511 Minimum temperatures during the winter were also accurately predicted, although the
512 temperatures in the deepest layer (75-100 cm) were overestimated by ~3°C in March. For
513 figure clarity we did not indicate the standard deviation of the observations, but provide
514 that information in Supplemental Material (Figure S5-S8).

Gautam Bisht 8/23/2017 5:29 AM
Deleted: material (Error! Reference source not found.).

Gautam Bisht 8/23/2017 5:29 AM
Deleted: ALMv0

515 Similarly, the soil temperatures were accurately predicted in the polygon rims
516 (Figure 5b). The largest discrepancies between measured and predicted soil temperatures
517 were in the shallowest layer (0 - 25 cm), where the predictions were up to a few °C cooler
518 than some of the observations between December 2012 and March 2013. In the polygon
519 center, a thicker snow pack acts as a heat insulator and keeps soil temperature higher in
520 winter as compared to the polygon rims.

Gautam Bisht 8/23/2017 5:29 AM
Deleted: ALMv0

Gautam Bisht 8/23/2017 5:29 AM
Deleted: (Error! Reference source not found. - Error! Reference source not found.).

521 Three recent studies have used other mechanistic models to simulate soil
522 temperature fields at this site, and achieved comparably good comparisons with
523 observations (Kumar et al. 2016 applied a 3D version of PFLOTRAN; Atchley et al. 2015 and
524 Harp et al. 2016 applied a 1D version of ATS). However, those models used measured soil

Gautam Bisht 8/23/2017 5:29 AM
Deleted: the

Gautam Bisht 8/23/2017 5:29 AM
Deleted: the

Gautam Bisht 8/23/2017 5:29 AM
Deleted: the

536 | temperatures near the surface as the top boundary condition. In contrast, the top boundary
537 condition in this work is the climate forcing (air temperature, wind, solar radiation,
538 humidity, precipitation), and the ground heat flux is prognosed based on ALM's vegetation
539 and surface energy dynamics. We note that no parameter calibration was done in this work
540 | or that of Kumar et al. (2016), while the ATS parameterizations were calibrated to match
541 the soil temperature profile.

Gautam Bisht 8/23/2017 5:29 AM

Deleted: temperature

542 Snow redistribution impacts spatial variability of soil temperature throughout the
543 soil column. Absence of SR results in no significant spatial variability of soil temperature
544 (Figure 6a). Inclusion of SR on the surface modifies the amount of energy exchanged
545 between the snow and the top soil layer, thereby creating spatial variability in the
546 temperature of the top soil, which propagates down into the soil column (Figure 6b). With
547 SR, energy dissipation in the lateral direction reduces the penetration depth of the soil
548 temperature spatial variance (compare Figure 6c and Figure 6b).

Gautam Bisht 8/23/2017 5:29 AM

Deleted: tuned

549 With 1D physics, the average spatial and temporal difference of the active layer
550 depth (ALD) between simulations with and without SR was 1.7 cm (Figure 7a), and the
551 absolute difference was 6.5 cm. As described above, we diagnosed the ALD to be the
552 maximum soil depth during the summer at which vertically interpolated soil temperature
553 is 0 °C. On average, the rims had ~10 cm shallower ALD with (blue line) than without
554 (green line) SR, consistent with the loss of insulation from SR on the rims during the
555 winter. In the centers (e.g., at location 42 - 55 m), the thaw depth was deeper by ~5 cm
556 with SR because of the higher snow depth there from SR. The effect of SR on the ALD was
557 largest on the rims because, compared to centers, they (1) on average lost more snow with
558 SR and (2) are more thermally conductive. Since rims are therefore colder at the time of
559 snowmelt with SR, the ground heat flux during the subsequent summer was unable to thaw
560 the soil column as deeply as when SR is ignored. For comparison, Atchley et al. (2015)
561 found in their sensitivity analysis using the 1D version of ATS that SR resulted in deeper
562 | thaw depths in both polygon centers (by ~3 cm) and rims (~0.3 cm). Thus, their results for
563 polygon centers are consistent in sign but lower in magnitude than ours, but opposite in
564 sign for the rims.

Gautam Bisht 8/23/2017 5:29 AM

Deleted: there

565 Across ten years of simulation, the inter-annual variability (IAV) in ALD varied
566 substantially between the three scenarios (Figure 7b). As expected, for the 1D physics

570 without SR scenario (green line), the IAV in ALD was determined by landscape position
571 because of differences in soil and vegetation parameters. With SR and 1D physics, the
572 model shows largest differences over the rims, again highlighting the relatively larger
573 effects of SR on the rim soil temperatures.

574 The effect of 1D versus 2D physics on the ALD across the transect was modest
575 (mean absolute difference ~ 3 cm). Generally, because 2D physics allows for lateral energy
576 diffusion, the horizontal variation of ALD was slightly lower (i.e., the red line is smoother
577 than the blue line; Figure 7a) than with 1D physics. This difference was also reflected in the
578 thaw depth IAV across the transect, where 2D physics led to a smoother lateral profile of
579 inter-annual variability than with 1D physics.

580 The impact of physics formulation (i.e., 1D or 2D) alone was investigated by
581 analyzing differences between soil temperature profiles over time for polygon rims and
582 centers in simulations with snow redistribution. Inclusion of 2D subsurface physics
583 resulted in soil temperatures with depth and time that were lower in the polygon rims
584 (Figure 8a) and higher in polygon centers (Figure 8b). Using the simulations from the
585 scenario with SR and 2D physics, we evaluated the extent to which soils under rims and
586 centers can be separately considered as relatively homogeneous single column systems by
587 evaluating the soil temperature standard deviation as a function of depth and time (Figure
588 9). During winter, both polygon rims and centers were predicted to have soil temperature
589 spatial variability > 1 °C up to a depth of ~ 2 m. The soil temperature spatial variability in
590 winter due to snow redistribution was dissipated over the summer. During the summer,
591 polygon centers were relatively more homogeneous vertically compared to polygon rims.

592 3.3 Surface Energy Budget

593 Predicted monthly- and spatial-mean (μ) surface latent heat fluxes across the
594 transect were very similar between the three scenarios (Figure 10a), with a growing
595 seasonal mean difference of < 1.0 $W m^{-2}$. However, the spatial variability ($SV = \sigma$; Figure
596 10b) and coefficient of variation ($CV = \sigma/\mu$; Figure 10c) of latent heat fluxes were different
597 between the scenarios with SR (1D and 2D physics) and without SR. With SR, the latent
598 heat flux spatial standard deviation peaked after snowmelt and declined until the fall when
599 snow began, from about $\sim 100\%$ to 10% of the mean. This relatively larger spatial variation

Gautam Bisht 8/23/2017 5:29 AM

Deleted: the

Gautam Bisht 8/23/2017 5:29 AM

Deleted: showed

Gautam Bisht 8/23/2017 5:29 AM

Deleted: [

Gautam Bisht 8/23/2017 5:29 AM

Deleted:].

Gautam Bisht 8/23/2017 5:29 AM

Deleted: is

Gautam Bisht 8/23/2017 5:29 AM

Deleted: season

Gautam Bisht 8/23/2017 5:29 AM

Deleted: [

Gautam Bisht 8/23/2017 5:29 AM

Deleted:].

608 in latent heat flux occurred because of large spatial heterogeneity in near surface soil
609 moisture in the beginning of summer, indicating a residual effect of SR from the previous
610 winter.

611 The predicted temporal monthly-mean and spatial-mean surface sensible heat
612 fluxes across the transect were also similar between the three scenarios (Figure 11a), with
613 a growing season mean absolute difference of $< 3.5 \text{ W m}^{-2}$. Also, the sensible heat flux
614 spatial variability differences occurred earlier than snowmelt, in contrast to the latent heat
615 flux. Both the standard deviation and CV of the sensible heat fluxes were larger than those
616 of the latent heat fluxes, with early season standard deviations of $\sim 50 \text{ W m}^{-2}$ (Figure 11b)
617 and CV's of ~ 1.5 (Figure 11c). As for the latent heat fluxes, the differences in standard
618 deviation and CV of sensible heat fluxes were small between the 1D and 2D scenarios with
619 SR, arguing that the subsurface lateral energy exchanges associated with the 2D physics did
620 not propagate to the mean surface heat fluxes. However, as for the latent heat flux, there
621 was a relatively large difference in spatial variation between the scenarios with and
622 without SR (e.g., of about 25 W m^{-2} in May; Figure 10b).

623 3.4 Soil Moisture

624 Neither SR nor 2D lateral physics affected the spatial mean moisture across time
625 (not shown). However, spatial heterogeneity of predicted soil moisture content differed
626 substantially between scenarios during the snow free period (Figure 12). For the 1D
627 simulations, the effect of SR was to increase growing season soil moisture spatial
628 heterogeneity by factors of 5.2 and 1.6 for 0-10 cm and 10-65 cm depth intervals,
629 respectively (compare Figure 12a and Figure 12b). Compared to 1D physics, simulating 2D
630 thermal and hydrologic physics led to an overall reduction in soil moisture spatial
631 heterogeneity by factors of 0.8 and 0.7 for 0-10 cm and 10-65 cm depth intervals,
632 respectively (compare Figure 12b and Figure 12c). Thus, with respect to dynamic spatial
633 mean soil moisture, SR effects dominated those associated with lateral subsurface water
634 movement.

Gautam Bisht 8/23/2017 5:29 AM

Deleted: the

Gautam Bisht 8/23/2017 5:29 AM

Deleted:

640 3.5 Caveats and Future Work

641 The good agreement between [ALM](#)-3D predictions and soil temperature
642 observations demonstrate the model's capabilities to represent this very spatially
643 heterogeneous and complex system. However, several caveats to our conclusions remain
644 due to uncertainties in model parameterizations, model structure, and climate forcing data.

645 [ALMv0, a one-dimensional model, is embarrassing parallel with no cross processor](#)
646 [communication. The current implementation of the three-dimensional solver in ALM-3D](#)
647 [only supports serial computing. Support of parallel computing will be included in a future](#)
648 [version of the model.](#) Because of computational constraints, we applied a 2D transect
649 domain to the site, instead of a full 3D domain. We are working to improve the
650 computational efficiency of the model, which will facilitate a thorough analysis of the
651 effects of 3D subsurface energy and water fluxes. A related issue is our simplified treatment
652 of surface water flows. A thorough analysis of the effects of surface water redistribution
653 would require integration of a 2D surface thermal flow model in a 3D domain, which is
654 another goal for our future work. However, we note that the good agreement using the 2D
655 model domain supports the idea that a two-dimensional simplification may be appropriate
656 for this system. The expected geomorphological changes in these systems over the coming
657 decades (e.g., Liljedahl et al. 2016), which will certainly affect soil temperature and
658 moisture, are not currently represented in ALM, although incorporation of these processes
659 is a long-term development goal.

660 The current representation of vegetation in [ALM](#)-3D for these polygonal tundra
661 systems is over-simplified. For example, non-vascular plants (mosses and lichens) are not
662 explicitly represented in the model, but can be responsible for a majority of evaporative
663 losses (Miller et al., 1976) and are strongly influenced by near surface hydrologic
664 conditions (Williams and Flanagan, 1996). Our use of the 'satellite phenology' mode, which
665 imposes transient LAI profiles for each plant functional type in the domain, ignores the
666 likely influence of nutrient constraints ([Zhu et al., 2016](#)) on photosynthesis and therefore
667 the surface energy budget. Other model simplifications, e.g., the simplified treatment of
668 radiation competition may also be important, especially as simulations are extended over
669 periods where vegetation change may occur (e.g., Grant 2016).

Gautam Bisht 8/23/2017 5:29 AM

Deleted: ALMv0

Gautam Bisht 8/23/2017 5:29 AM

Deleted: with the ALMv0-3D

Gautam Bisht 8/23/2017 5:29 AM

Deleted: ALMv0

Gautam Bisht 8/23/2017 5:29 AM

Deleted: (Zhu et al., 2016a)

674 Development of sub grid parameterizations to parsimoniously capture fine scale
675 processes will be pursued in the future. For example, a two-tile approach to represent
676 hydrologic and thermal processes in coupled polygon rims and centers with snow
677 redistribution should be evaluated. Inclusion of lateral subsurface processes has a greater
678 impact on predicted subgrid variability than on spatially averaged states. Thus, one
679 possible extension of the current model would be to explicitly include an equation for the
680 temporal evolution of sub grid variability using the approach of Montaldo and Albertson
681 (2003). The use of reduced-order models (e.g., Pau et al. (2014); Liu et al. (2016)) is an
682 alternate approach to estimate fine scale hydrologic and thermal states from a coarse
683 resolution representation. Additionally, lateral subsurface processes can be included in the
684 land surface model via a range of numerical discretization approaches of varying
685 complexity, e.g., adding lateral water and energy fluxes as source/sink terms in the existing
686 1D model, implementing an operator split approach to solve vertical and lateral processes
687 in a non-iterative approach, or solving a fully coupled 3D model. Tradeoffs between various
688 approaches to include lateral processes and computational needs to be carefully studied
689 before developing quasi or fully three-dimensional land surface models. While the present
690 study focused on application and validation of ALM-3D at fine-scale, future work will focus
691 on regional scale applications using comprehensive datasets and modeling protocol of the
692 Distributed Model Intercomparison Project Phase 2 (Smith et al., 2012)

693 4 Summary and Conclusions

694 In a polygonal tundra landscape, we analyzed effects of microtopographical surface
695 heterogeneity and lateral subsurface transport on soil temperature, soil moisture, and
696 surface energy exchanges. Starting from the climate-scale land model ALMv0, we
697 incorporated in ALM-3D numerical representations of subsurface water and energy lateral
698 transport that are solved using PETSc. A simple method for redistributing incoming snow
699 along the microtopographic transect was also integrated in the model.

700 Over the observational record, ALM-3D with snow redistribution and lateral heat
701 and hydrological fluxes accurately predicted snow depth and soil temperature vertical
702 profiles in the polygon rims and centers (overall bias, RMSE, and R^2 of 0.59°C, 1.82°C and

Gautam Bisht 8/23/2017 5:29 AM

Deleted: We

Gautam Bisht 8/23/2017 5:29 AM

Deleted: the

Gautam Bisht 8/23/2017 5:29 AM

Deleted: in a polygonal tundra landscape

Gautam Bisht 8/23/2017 5:29 AM

Deleted: ALMv0

Gautam Bisht 8/23/2017 5:29 AM

Deleted: ALMv0

708 0.99, respectively). In the rims, the transition to thawed soil in spring, summer
709 temperature dynamics, and minimum temperatures during the winter were all accurately
710 predicted. In the centers, a $\sim 2^\circ\text{C}$ warm bias in April in the 75-100 cm soil layer was
711 predicted, although this bias disappeared during snowmelt.

712 The spatial heterogeneity of snow depth during the winter due to snow
713 redistribution generated surface soil temperature heterogeneity that propagated into the
714 soil over time. The temporal and spatial variation of snow depth was affected by snow
715 redistribution, but not by lateral thermal and hydrologic transport. Both snow
716 redistribution and lateral thermal fluxes affected spatial variability of soil temperatures.
717 Energy dissipation in the lateral direction reduced the depth to which soil temperature
718 variance penetrated. Snow redistribution led to ~ 10 cm shallower active layer depths
719 under the polygon rims because of the residual effect of reduced insulation during the
720 winter. In contrast, snow redistribution led to ~ 5 cm deeper maximum thaw depth under
721 the polygon centers. The effect of lateral energy fluxes on active layer depths was ~ 3 cm.
722 Compared to 1D physics, the 2D subsurface physics led to lower (higher) soil temperatures
723 with depth and time in the polygon rims (centers). The larger than 1°C wintertime spatial
724 temperature variability down to ~ 2 m depth in rims and centers indicates the uncertainty
725 associated with considering rims and centers as separate 1D columns. During the summer,
726 polygon center temperatures were relatively more vertically homogeneous than
727 temperatures in the rims.

728 The monthly- and spatial-mean predicted latent and sensible heat fluxes were
729 unaffected by snow redistribution and lateral heat and hydrological fluxes. However, snow
730 redistribution led to spatial heterogeneity in surface energy fluxes and soil moisture during
731 the summer. Excluding lateral subsurface hydrologic and thermal processes led to an over
732 prediction of spatial variability in soil moisture and soil temperature because subsurface
733 gradients were artificially prevented from laterally dissipating over time. Snow
734 redistribution effects on soil moisture heterogeneity were larger than those associated
735 with lateral thermal fluxes.

736 Overall, our analysis demonstrates the potential and value of explicitly representing
737 snow redistribution and lateral subsurface hydrologic and thermal dynamics in polygonal
738 ground systems and quantifies the effects of these processes on the resulting system states

Gautam Bisht 8/23/2017 5:29 AM

Deleted: active layers

Gautam Bisht 8/23/2017 5:29 AM

Deleted:

741 | and surface energy exchanges with the atmosphere. The integration of a 3D subsurface
742 | model in the ACME Land Model also allows for a wide range of analyses heretofore
743 | impossible in an Earth System Model context.

744 |

Gautam Bisht 8/23/2017 5:29 AM

Deleted: processes

746 **5 Code availability**

747 The ALM-3D v1.0 code and data used in study are publicly available at

748 <https://bitbucket.org/gbisht/lateral-subsurface-model> and

749 <https://bitbucket.org/gbisht/notes-for-gmd-2017-71>.

750

Gautam Bisht 8/23/2017 5:29 AM

Formatted: Normal, Left

751 **6 Tables**

752 **Table 1. Bias, root mean square error (RMSE), and correlation (R^2) between modeled and**
 753 **observed snow depth at polygon center, rim and difference between center and rim for**
 754 **2013 for three cases: Snow redistribution (SR) off and 1D physics, SR on and 1D physics,**
 755 **and SR on and 2D physics.**

	SR=Off, Physics=1D			SR=On, Physics=1D			SR=On, Physics=2D		
	Center	Rim	Center-Rim	Center	Rim	Center-Rim	Center	Rim	Center-Rim
Bias	-0.08	0.02	-0.10	-0.04	-0.03	-0.02	-0.04	-0.03	-0.02
RMSE	0.12	0.04	0.12	0.08	0.04	0.05	0.08	0.04	0.05
R^2	0.86	0.92	0.03	0.78	0.85	0.73	0.79	0.85	0.73

756

757

Gautam Bisht 8/23/2017 5:29 AM
 Deleted: 1

759 **Table 2 Bias, root mean square error (RMSE) and correlation (R^2) between modeled and**
 760 **observed soil temperature at polygon center and rim at multiple soil depth for 2013 for**
 761 **three cases: Snow redistribution (SR) off and 1D physics, SR on and 1D physics, and SR on**
 762 **and 2D physics.**

Bias						
	SR=Off, Physics=1D		SR=On, Physics=2D		SR=On, Physics=2D	
Depth [m]	Center	Rim	Center	Rim	Center	Rim
0.00 - 0.20	0.86	-1.73	-0.19	1.00	0.52	0.71
0.20 - 0.50	0.68	-1.52	-0.46	0.98	0.35	0.62
0.50 - 0.75	0.53	-1.49	-0.64	0.94	0.21	0.53
0.75 - 1.00	0.49	-1.44	-0.67	-0.97	0.22	0.49
Average across four depths	0.64	-1.54	-0.49	0.97	0.33	0.59

763

RMSE						
	SR=Off, Physics=1D		SR=On, Physics=2D		SR=On, Physics=2D	
Depth [m]	Center	Rim	Center	Rim	Center	Rim
0.00 - 0.20	2.11	3.39	2.20	2.94	1.90	2.66
0.20 - 0.50	1.49	2.73	1.39	1.86	1.12	1.57
0.50 - 0.75	1.60	2.42	1.22	1.96	1.14	1.60
0.75 - 1.00	1.50	2.15	1.12	1.87	1.09	1.44
Average across four depths	1.67	2.67	1.44	2.16	1.31	1.82

764

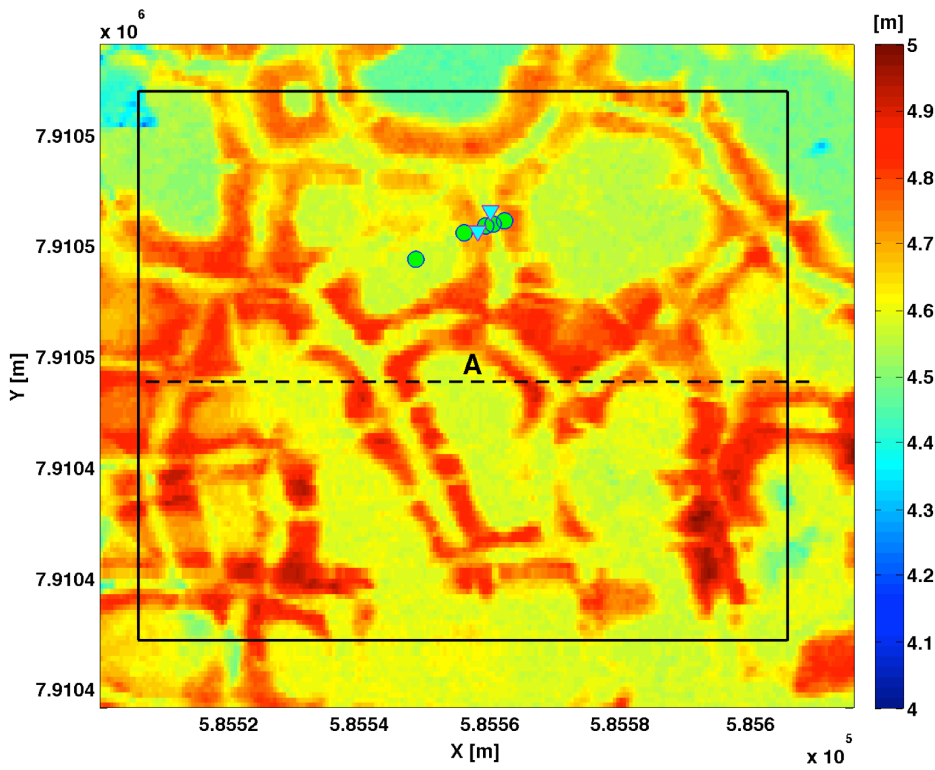
R^2						
	SR=Off, Physics=1D		SR=On, Physics=2D		SR=On, Physics=2D	
Depth [m]	Center	Rim	Center	Rim	Center	Rim
0.00 - 0.20	0.98	0.95	0.97	0.97	0.98	0.97

0.20 - 0.50	0.99	0.96	0.98	0.99	0.99	0.99
0.50 - 0.75	0.99	0.97	0.99	0.99	1.00	0.99
0.75 - 1.00	0.99	0.97	0.99	0.99	1.00	0.99
Average across four depths	0.99	0.96	0.98	0.99	0.99	0.99

765

766

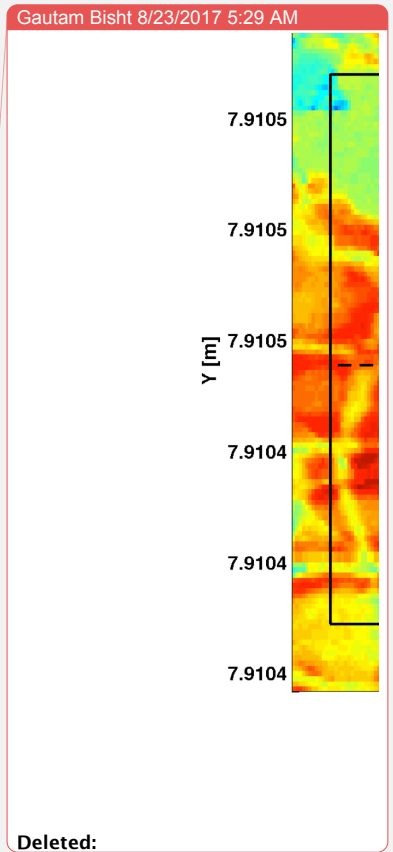
767 **7 Figures**

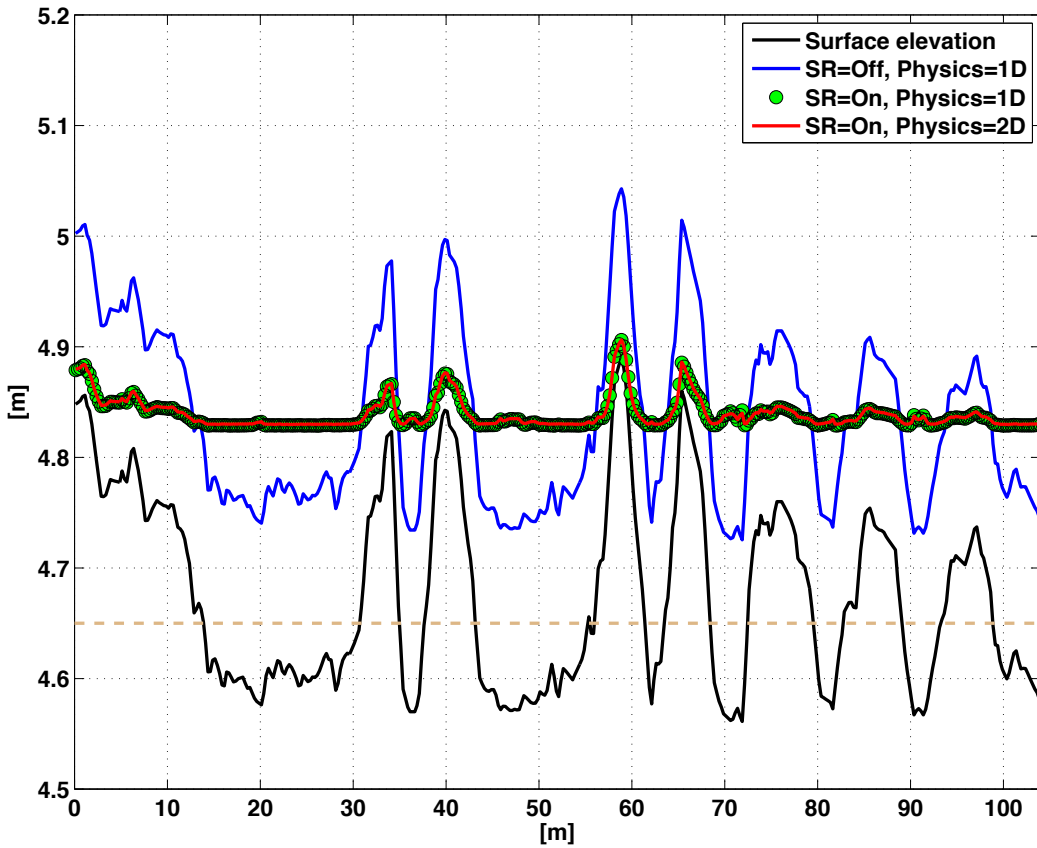


768

769 **Figure 1** The NGEE-Arctic study area A, which characterized as a low-centered polygon
770 field. Dotted line indicate the transect along which simulation in this paper are preformed
771 to demonstrate the effects of snow redistribution on soil temperature. The locations where
772 snow and temperature sensors are installed within the study site are denoted by triangle
773 and circle, respectively.

774

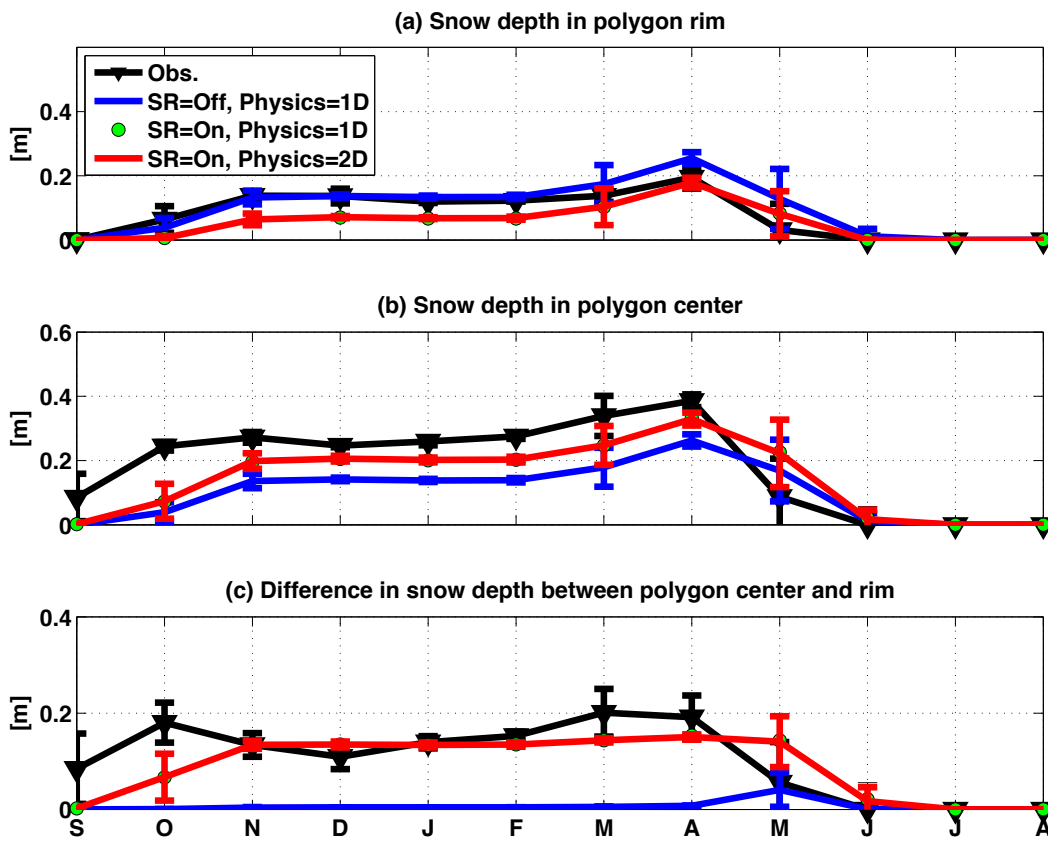




776
 777 **Figure 2. Simulated average winter snow surface elevation across the transect for three**
 778 **scenarios: (1) snow redistribution (SR) turned off and 1D subsurface physics, (2) snow**
 779 **redistribution turned on and 1D subsurface physics, and (3) snow redistribution turned on**
 780 **and 2D subsurface physics. Surface elevation of the transect is shown by solid black line.**
 781 **The dashed line indicates the boundary for comparison to observations in relatively lower**
 782 **(centers) and relatively higher (ridges) topographical positions.**

783

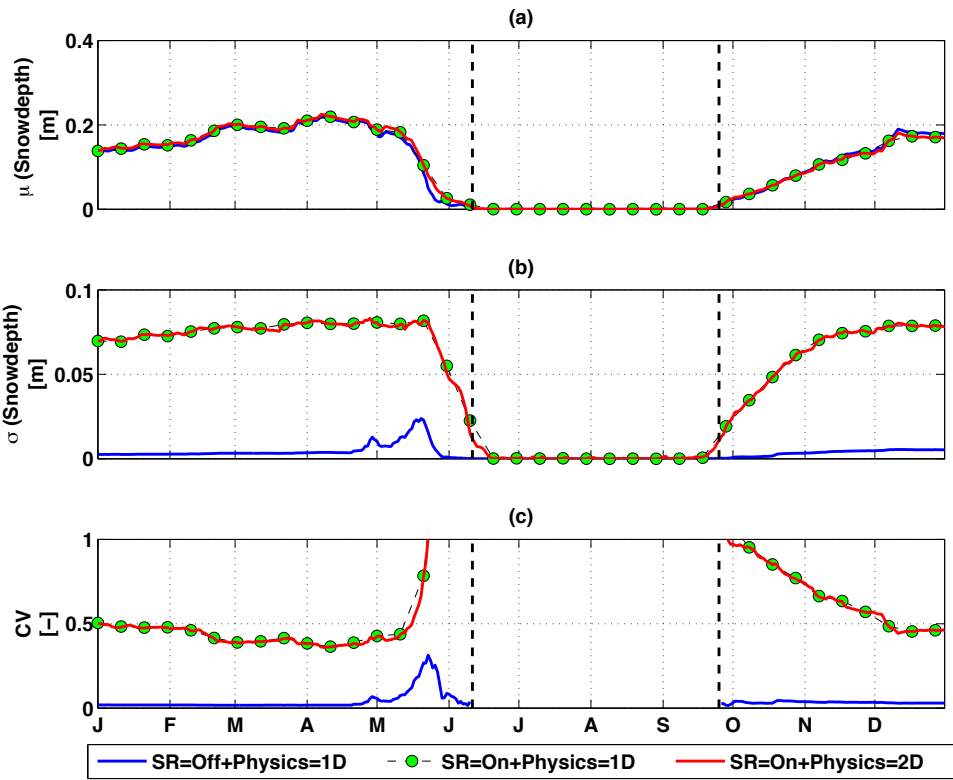
784



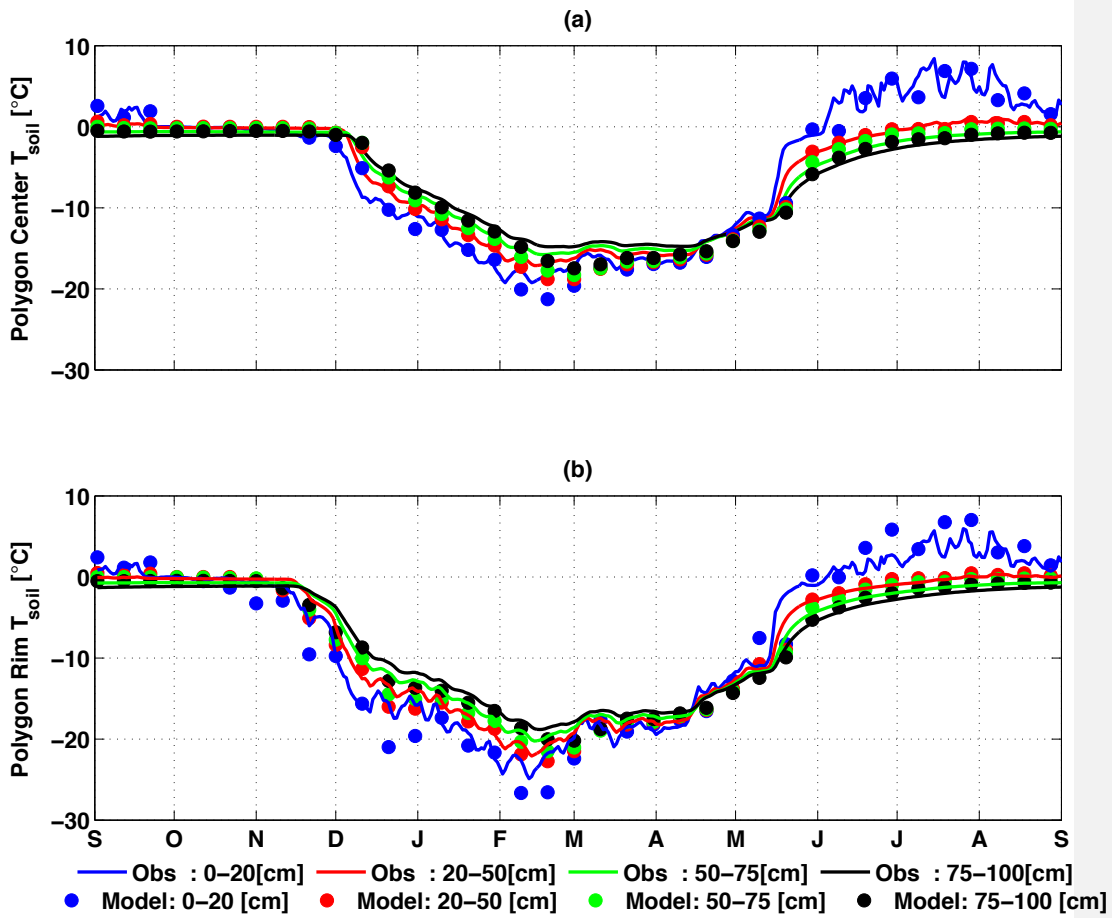
785

786

787 **Figure 3** Monthly-mean comparison of observation and simulated snow depth (a) in
788 polygon rim, (b) in polygon center; (c) difference between polygon center and rim for 2013.

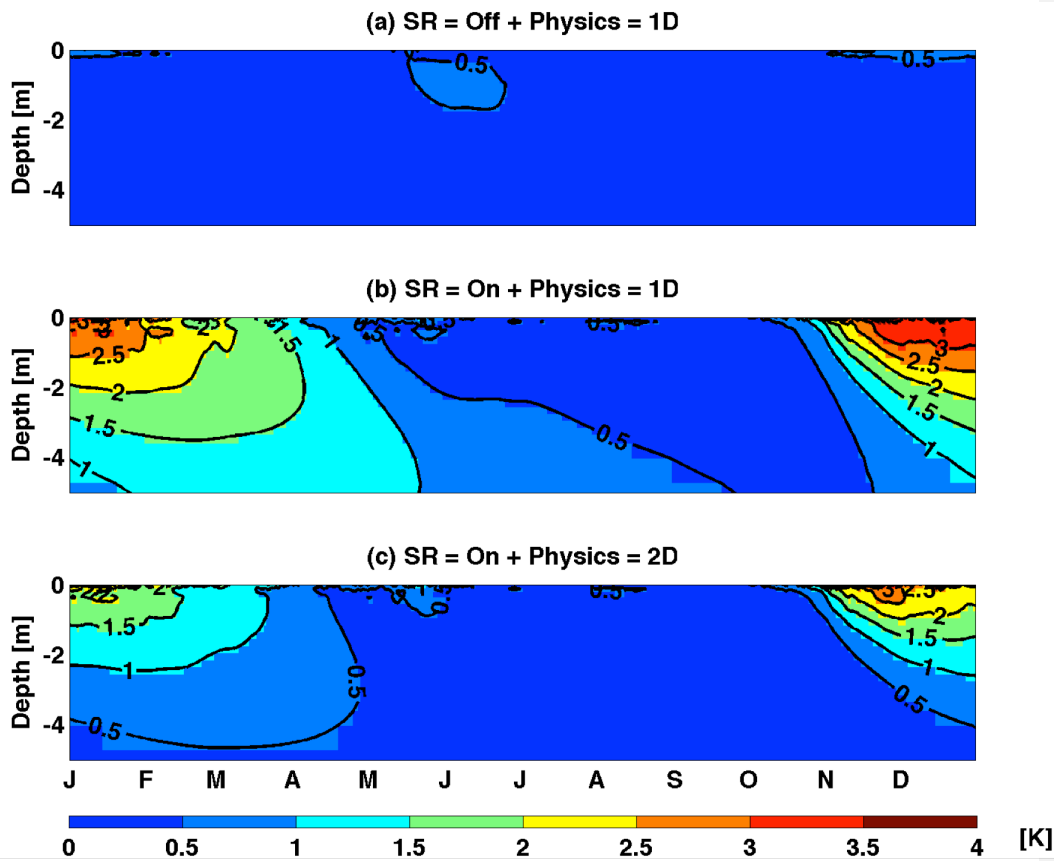


789
 790 **Figure 4. Mean, standard deviation and coefficient of variation of simulated snow**
 791 **depth across the entire domain for 1D and 2D subsurface physics.**



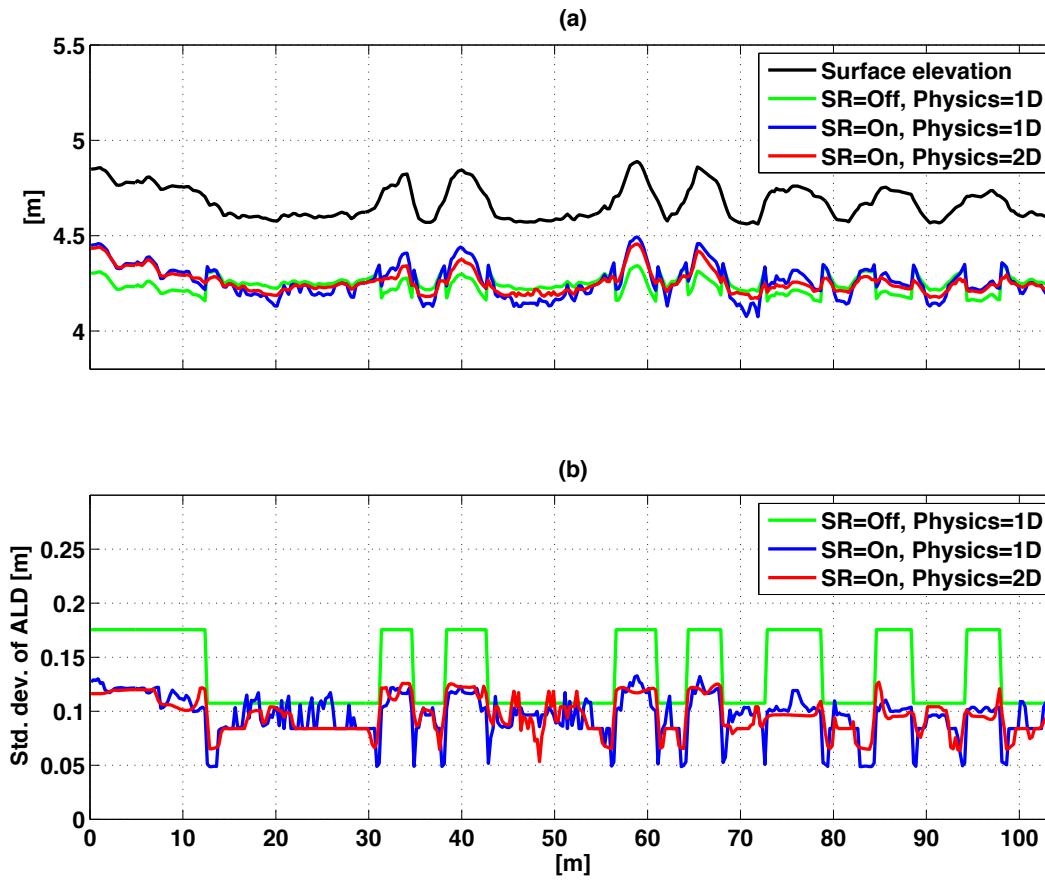
792
 793 **Figure 5 Comparison of soil temperature observations and predictions in polygon centers**
 794 **(a) and rims (b). Simulation was performed with snow redistribution on and 2D subsurface**
 795 **physics, between September 2012 and September 2013. Simulation results are shown at an**
 796 **interval of 10 days, while observations are shown at daily interval**

797
 798



799
 800 **Figure 6 Simulated daily spatial standard deviation averaged across 10-year of near**
 801 **surface soil temperature for simulation performed with snow redistribution turned off and**
 802 **1D subsurface physics (top panel); snow redistribution turned on and 1D subsurface**
 803 **physics (middle panel); and snow redistribution turned on and 2D subsurface physics**
 804 **(bottom panel).**

805
 806

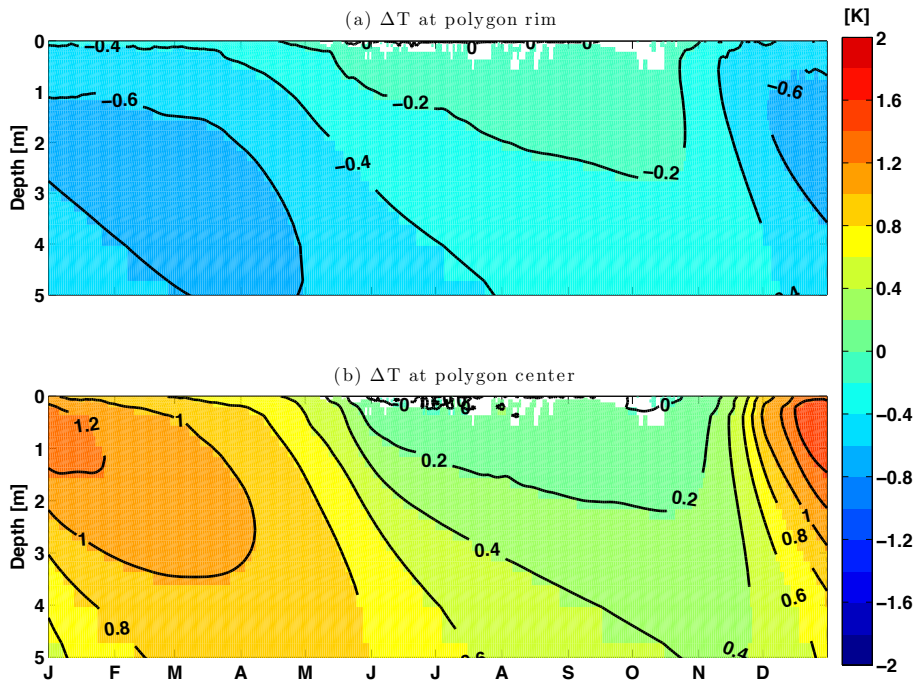


807
 808
 809 **Figure 7** Temporal mean of the bottom of the active layer (top panel) and standard
 810 deviation of the active layer depth (bottom panel) over the 10-year period across the
 811 modeling domain.

812

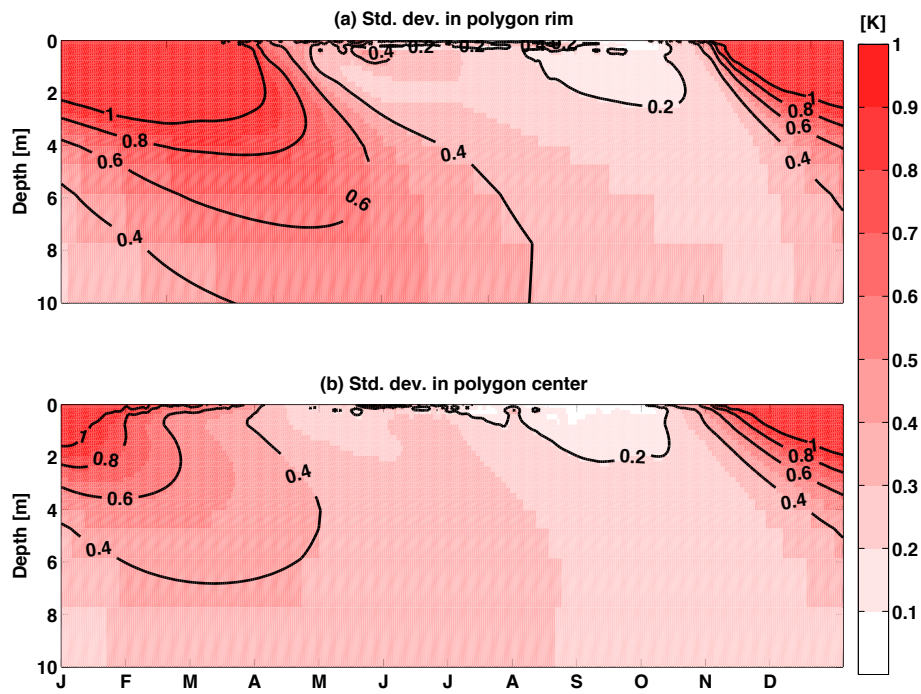
813

814

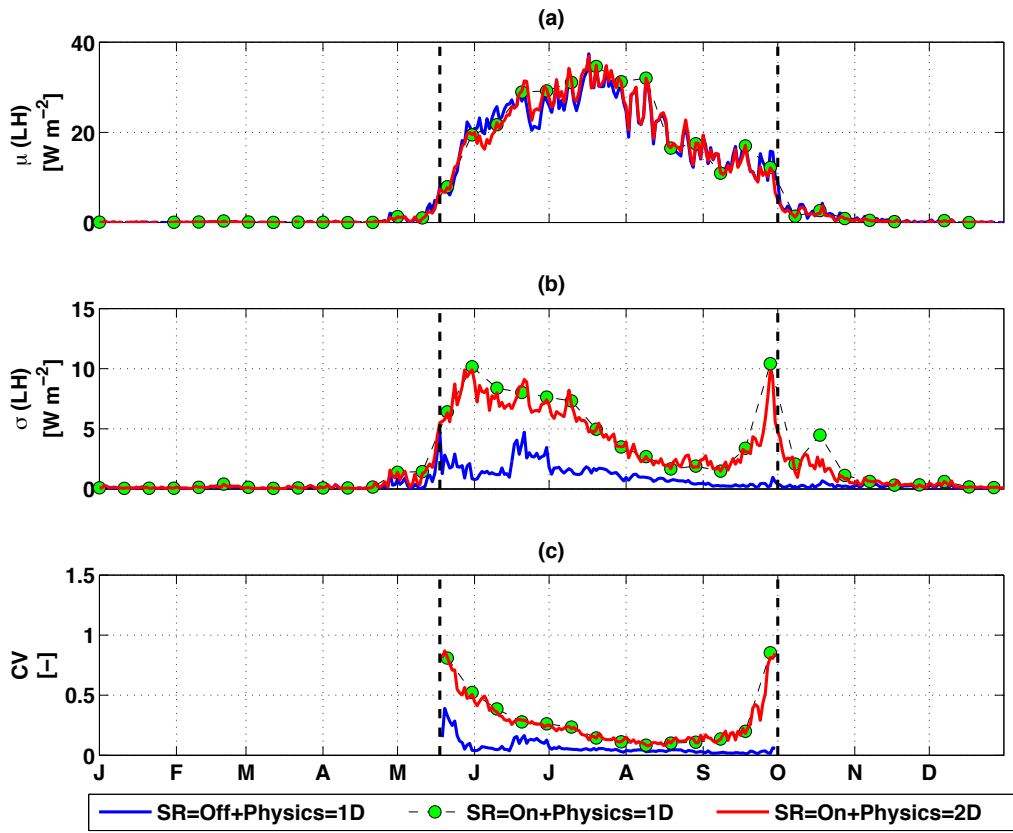


815

816 **Figure 8** Time series of spatial mean soil temperature differences between “SR=On +
817 **Physics=1D**” and “SR=On + Physics=2D” at polygon rim (top panel) and polygon center
818 **(bottom panel).**



819
 820 **Figure 9 Time series of soil temperature spatial standard deviation for “SR=On +**
 821 **Physics=2D” at polygon rim (top panel) and polygon center (bottom panel).**



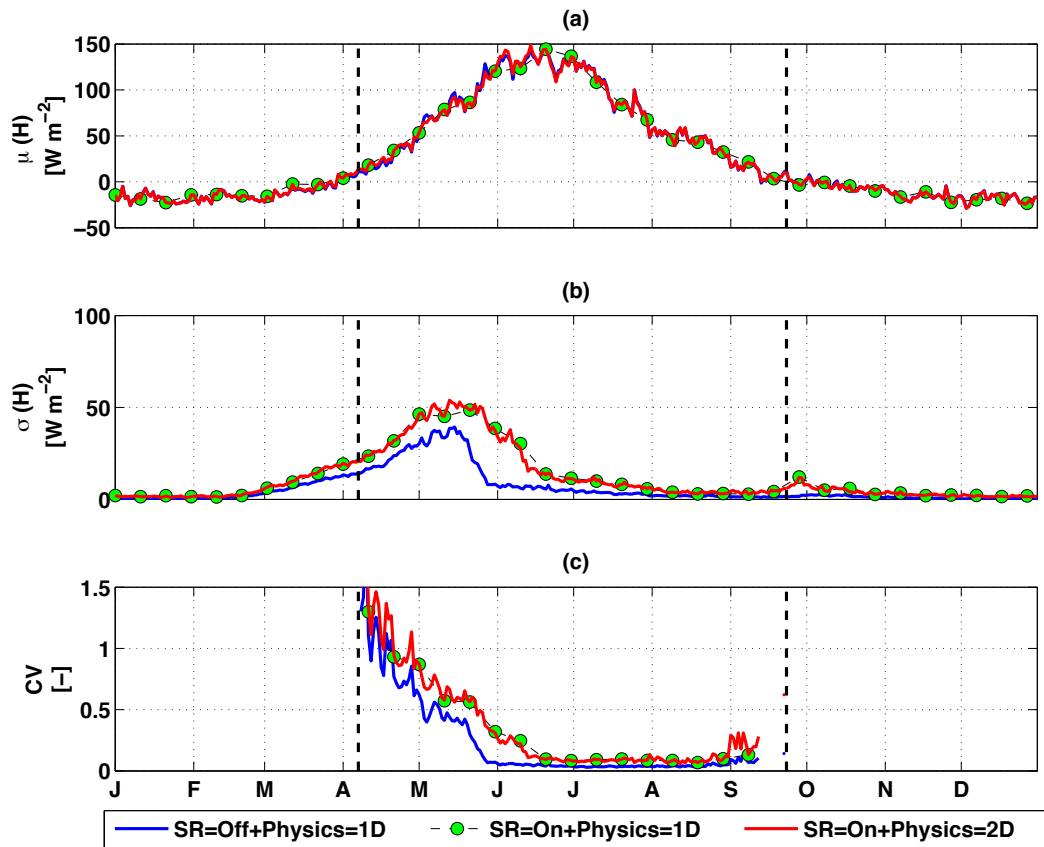
822

823

824 **Figure 10. Latent heat flux inter-annual (a) mean, (b) standard deviation, and (c)**

825 **coefficient of variation across the site A transect.**

826

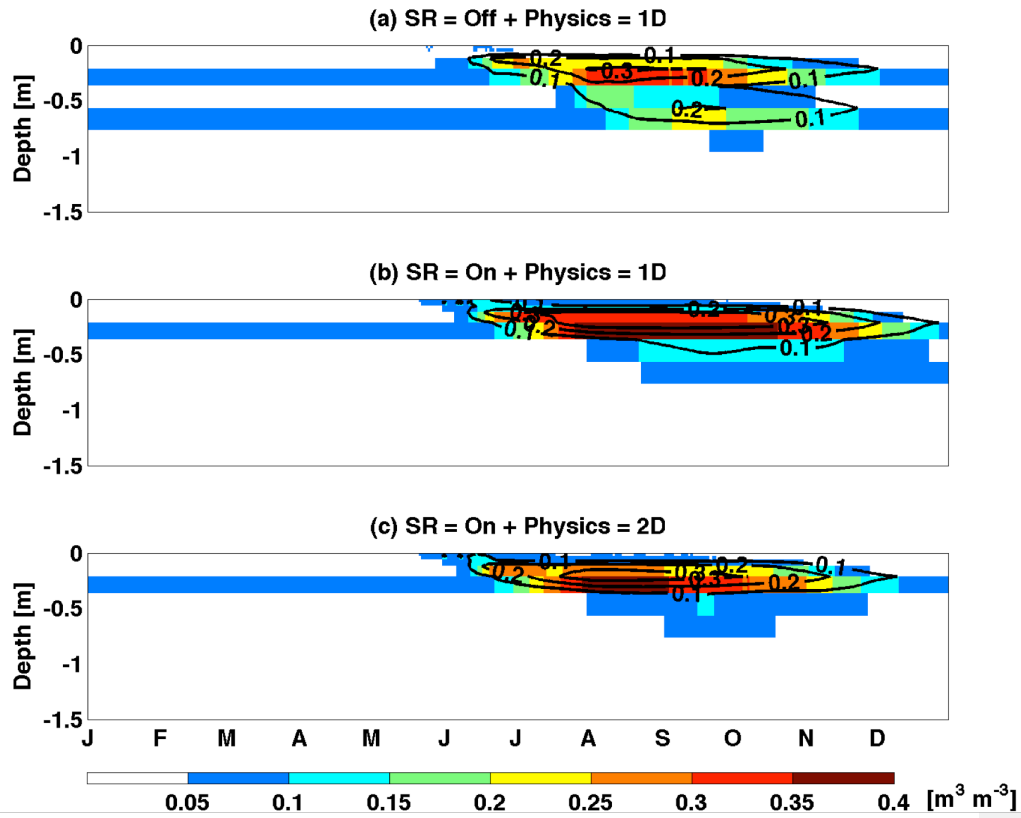


827

828

829 Figure 11. Same as Figure 10 except for sensible heat flux.

830



831

832 Figure 12. Same as Figure 6 except for liquid saturation.

833 **Acknowledgements.**

834 This research was supported by the Director, Office of Science, Office of Biological and
835 Environmental Research of the US Department of Energy under Contract No. DE-AC02-
836 05CH11231 as part of the NGEE-Arctic and Accelerated Climate Modeling for Energy (ACME)
837 programs.

838 **References**

839 Anderson, E. A.: A point energy and mass balance model of a snow cover, National Weather
840 Service, Silver Spring, MD, 1976.

841 Balay, S., Abhyankar, S., Adams, M. F., Brown, J., Brune, P., Buschelman, K., Dalcin, L.,
842 Eijkhout, V., Gropp, W. D., Kaushik, D., Knepley, M. G., McInnes, L. C., Rupp, K., Smith, B.
843 F., Zampini, S., Zhang, H., and Zhang, H.: PETSc Users Manual, Argonne National Laboratory,
844 2016.

845 Bartelt, P. and Lehning, M.: A physical SNOWPACK model for the Swiss avalanche warning:
846 Part I: numerical model, Cold Regions Science and Technology, 35, 123-145, 2002.

847 Borner, A. P., Kielland, K., and Walker, M. D.: Effects of Simulated Climate Change on Plant
848 Phenology and Nitrogen Mineralization in Alaskan Arctic Tundra, Arctic, Antarctic, and Alpine
849 Research, 40, 27-38, 2008.

850 Callaghan, T., Johansson, M., Brown, R., Groisman, P., Labba, N., Radionov, V., Barry, R.,
851 Bulygina, O., Essery, R. H., Frolov, D. M., Golubev, V., Grenfell, T., Petrushina, M., Razuvaev,
852 V., Robinson, D., Romanov, P., Shindell, D., Shmakin, A., Sokratov, S., Warren, S., and Yang,
853 D.: The Changing Face of Arctic Snow Cover: A Synthesis of Observed and Projected Changes,
854 AMBIO, 40, 17-31, 2011a.

855 Callaghan, T., Johansson, M., Brown, R., Groisman, P., Labba, N., Radionov, V., Bradley, R.,
856 Blangy, S., Bulygina, O., Christensen, T., Colman, J., Essery, R. H., Forbes, B., Forchhammer,
857 M., Golubev, V., Honrath, R., Juday, G., Meshcherskaya, A., Phoenix, G., Pomeroy, J., Rautio,
858 A., Robinson, D., Schmidt, N., Serreze, M., Shevchenko, V., Shiklomanov, A., Shmakin, A.,
859 Sköld, P., Sturm, M., Woo, M.-k., and Wood, E.: Multiple Effects of Changes in Arctic Snow
860 Cover, AMBIO, 40, 32-45, 2011b.

861 Clark, M. P., Hendrikx, J., Slater, A. G., Kavetski, D., Anderson, B., Cullen, N. J., Kerr, T., Örn
862 Hreinsson, E., and Woods, R. A.: Representing spatial variability of snow water equivalent in
863 hydrologic and land-surface models: A review, Water Resources Research, 47, W07539, 2011.

864 Cox, P. M., Betts, R. A., Jones, C. D., Spall, S. A., and Totterdell, I. J.: Acceleration of global
865 warming due to carbon-cycle feedbacks in a coupled climate model, Nature, 408, 184-187, 2000.

866 Dai, Y. and Zeng, Q.: A land surface model (IAP94) for climate studies part I: Formulation and
867 validation in off-line experiments, Advances in Atmospheric Sciences, 14, 433-460, 1997.

Gautam Bisht 8/23/2017 5:29 AM

Deleted: Barber, V. A., Juday, G. P., and Finney, B. P.: Reduced growth of Alaskan white spruce in the twentieth century from temperature-induced drought stress, Nature, 405, 668-673, 2000. .

Gautam Bisht 8/23/2017 5:29 AM

Deleted: Chapin, F. S., Shaver, G. R., Giblin, A. E., Nadelhoffer, K. J., and Laundre, J. A.: Responses of Arctic Tundra to Experimental and Observed Changes in Climate, Ecology, 76, 694-711, 1995. .

Gautam Bisht 8/23/2017 5:29 AM

Deleted: Cornelissen, J. H. C., Callaghan, T. V., Alatalo, J. M., Michelsen, A., Graglia, E., Hartley, A. E., Hik, D. S., Hobbie, S. E., Press, M. C., Robinson, C. H., Henry, G. H. R., Shaver, G. R., Phoenix, G. K., Gwynn Jones, D., Jonasson, S., Chapin, F. S., Molau, U., Neill, C., Lee, J. A., Melillo, J. M., Sveinbjörnsson, B., and Aerts, R.: Global change and arctic ecosystems: is lichen decline a function of increases in vascular plant biomass?, Journal of Ecology, 89, 984-994, 2001. .

890 | Dufresne, J. L., Fairhead, L., Le Treut, H., Berthelot, M., Bopp, L., Ciais, P., Friedlingstein, P.,
891 | and Monfray, P.: On the magnitude of positive feedback between future climate change and the
892 | carbon cycle, *Geophysical Research Letters*, 29, 43-41-43-44, 2002.

893 | Engstrom, R., Hope, A., Kwon, H., Stow, D., and Zamolodchikov, D.: Spatial distribution of
894 | near surface soil moisture and its relationship to microtopography in the Alaskan Arctic coastal
895 | plain, *Nordic Hydrology*, 36, 219-234, 2005.

896 | Euskirchen, E. S., McGuire, A. D., Chapin, F. S., Yi, S., and Thompson, C. C.: Changes in
897 | vegetation in northern Alaska under scenarios of climate change, 2003–2100: implications for
898 | climate feedbacks, *Ecological Applications*, 19, 1022-1043, 2009.

899 | Frey, S. and Holzmann, H.: A conceptual, distributed snow redistribution model, *Hydrol. Earth*
900 | *Syst. Sci.*, 19, 4517-4530, 2015.

901 | Friedlingstein, P., Bopp, L., Ciais, P., Dufresne, J.-L., Fairhead, L., LeTreut, H., Monfray, P.,
902 | and Orr, J.: Positive feedback between future climate change and the carbon cycle, *Geophysical*
903 | *Research Letters*, 28, 1543-1546, 2001.

904 | Friedlingstein, P., Cox, P., Betts, R., Bopp, L., von Bloh, W., Brovkin, V., Cadule, P., Doney, S.,
905 | Eby, M., Fung, I., Bala, G., John, J., Jones, C., Joos, F., Kato, T., Kawamiya, M., Knorr, W.,
906 | Lindsay, K., Matthews, H. D., Raddatz, T., Rayner, P., Reick, C., Roeckner, E., Schnitzler, K.
907 | G., Schnur, R., Strassmann, K., Weaver, A. J., Yoshikawa, C., and Zeng, N.: Climate–Carbon
908 | Cycle Feedback Analysis: Results from the C4MIP Model Intercomparison, *Journal of Climate*,
909 | 19, 3337-3353, 2006.

910 | Fung, I. Y., Doney, S. C., Lindsay, K., and John, J.: Evolution of carbon sinks in a changing
911 | climate, *Proceedings of the National Academy of Sciences of the United States of America*, 102,
912 | 11201-11206, 2005.

913 | Galen, C. and Stanton, M. L.: Responses of Snowbed Plant Species to Changes in Growing-
914 | Season Length, *Ecology*, 76, 1546-1557, 1995.

915 | Ghimire, B., Riley, W. J., Koven, C. D., Mu, M., and Randerson, J. T.: Representing leaf and
916 | root physiological traits in CLM improves global carbon and nitrogen cycling predictions,
917 | *Journal of Advances in Modeling Earth Systems*, 8, 598-613, 2016.

918 | Govindasamy, B., Thompson, S., Mirin, A., Wickett, M., Caldeira, K., and Delire, C.: Increase
919 | of carbon cycle feedback with climate sensitivity: results from a coupled climate and carbon
920 | cycle model, *Tellus B*, 57, 2011.

Gautam Bisht 8/23/2017 5:29 AM

Deleted: Davidson, E. A. and Janssens, I. A.: Temperature sensitivity of soil carbon decomposition and feedbacks to climate change, *Nature*, 440, 165-173, 2006. -

Gautam Bisht 8/23/2017 5:29 AM

Deleted: Euskirchen, E. S., McGuire, A. D., Kicklighter, D. W., Zhuang, Q., Clein, J. S., Dargaville, R. J., Dye, D. G., Kimball, J. S., McDonald, K. C., Melillo, J. M., Romanovsky, V. E., and Smith, N. V.: Importance of recent shifts in soil thermal dynamics on growing season length, productivity, and carbon sequestration in terrestrial high-latitude ecosystems, *Global Change Biology*, 12, 731-750, 2006. -

935 Groendahl, L., Friberg, T., and Soegaard, H.: Temperature and snow-melt controls on
936 interannual variability in carbon exchange in the high Arctic, *Theoretical and Applied*
937 *Climatology*, 88, 111-125, 2007.

938 Grogan, P. and Chapin Iii, F. S.: Arctic Soil Respiration: Effects of Climate and Vegetation
939 Depend on Season, *Ecosystems*, 2, 451-459, 1999.

940 Hartman, M. D., Baron, J. S., Lammers, R. B., Cline, D. W., Band, L. E., Liston, G. E., and
941 Tague, C.: Simulations of snow distribution and hydrology in a mountain basin, *Water Resources*
942 *Research*, 35, 1587-1603, 1999.

943 Helfricht, K., Schöber, J., Seiser, B., Fischer, A., Stötter, J., and Kuhn, M.: Snow accumulation
944 of a high alpine catchment derived from LiDAR measurements, *Adv. Geosci.*, 32, 31-39, 2012.

945 Hinkel, K. M., Eisner, W. R., Bockheim, J. G., Nelson, F. E., Peterson, K. M., and Dai, X.:
946 Spatial Extent, Age, and Carbon Stocks in Drained Thaw Lake Basins on the Barrow Peninsula,
947 Alaska, *Arctic, Antarctic and Alpine Research*, 35, 291-300, 2003.

948 Hinkel, K. M., Frohn, R. C., Nelson, F. E., Eisner, W. R., and Beck, R. A.: Morphometric and
949 spatial analysis of thaw lakes and drained thaw lake basins in the western Arctic Coastal Plain,
950 Alaska, *Permafrost and Periglacial Processes*, 16, 327-341, 2005.

951 Hinzman, L. D. and Kane, D. L.: Potential response of an Arctic watershed during a period of
952 global warming, *Journal of Geophysical Research: Atmospheres*, 97, 2811-2820, 1992.

953 | Holland, M. M. and Bitz, C. M.: Polar amplification of climate change in coupled models,
954 *Climate Dynamics*, 21, 221-232, 2003.

955 | Jiang, D., Zhang, Y., and Lang, X.: Vegetation feedback under future global warming,
956 *Theoretical and Applied Climatology*, 106, 211-227, 2011.

957 Jones, C. D., Cox, P. M., Essery, R. L. H., Roberts, D. L., and Woodage, M. J.: Strong carbon
958 cycle feedbacks in a climate model with interactive CO₂ and sulphate aerosols, *Geophysical*
959 *Research Letters*, 30, 1479, 2003.

960 Jones, H. G.: The ecology of snow-covered systems: a brief overview of nutrient cycling and life
961 in the cold, *Hydrological Processes*, 13, 2135-2147, 1999.

962 Jordan, R. E.: One-dimensional temperature model for a snow cover : technical documentation
963 for SNTHERM.89, Cold Regions Research and Engineering Laboratory (U.S.) Engineer
964 Research and Development Center (U.S.), 1991.

Gautam Bisht 8/23/2017 5:29 AM

Deleted: Hobbie, S. E.: Temperature and Plant Species Control Over Litter Decomposition in Alaskan Tundra, *Ecological Monographs*, 66, 503-522, 1996. - Hollister, R. D., Webber, P. J., and Bay, C.: PLANT RESPONSE TO TEMPERATURE IN NORTHERN ALASKA: IMPLICATIONS FOR PREDICTING VEGETATION CHANGE, *Ecology*, 86, 1562-1570, 2005. -

Gautam Bisht 8/23/2017 5:29 AM

Deleted: Hollister, R. D., Webber, P. J., and Bay, C.: PLANT RESPONSE TO TEMPERATURE IN NORTHERN ALASKA: IMPLICATIONS FOR PREDICTING VEGETATION CHANGE, *Ecology*, 86, 1562-1570, 2005. -

981 Jorgenson, M. T., Shur, Y. L., and Pullman, E. R.: Abrupt increase in permafrost degradation in
982 Arctic Alaska, *Geophysical Research Letters*, 33, L02503, 2006.

983 Koven, C. D., Lawrence, D. M., and Riley, W. J.: Permafrost carbon–climate feedback is
984 sensitive to deep soil carbon decomposability but not deep soil nitrogen dynamics, *Proceedings*
985 *of the National Academy of Sciences*, 112, 3752-3757, 2015.

986 Koven, C. D., Riley, W. J., Subin, Z. M., Tang, J. Y., Torn, M. S., Collins, W. D., Bonan, G. B.,
987 Lawrence, D. M., and Swenson, S. C.: The effect of vertically resolved soil biogeochemistry and
988 alternate soil C and N models on C dynamics of CLM4, *Biogeosciences*, 10, 7109-7131, 2013.

989 Koven, C. D., Ringeval, B., Friedlingstein, P., Ciais, P., Cadule, P., Khvorostyanov, D., Krinner,
990 G., and Tarnocai, C.: Permafrost carbon-climate feedbacks accelerate global warming,
991 *Proceedings of the National Academy of Sciences*, 108, 14769-14774, 2011.

992 Lawrence, D. M. and Swenson, S. C.: Permafrost response to increasing Arctic shrub abundance
993 depends on the relative influence of shrubs on local soil cooling versus large-scale climate
994 warming, *Environmental Research Letters*, 6, 045504, 2011.

995 Liston, G. E. and Elder, K.: A Distributed Snow-Evolution Modeling System (SnowModel),
996 *Journal of Hydrometeorology*, 7, 1259-1276, 2006.

997 Liston, G. E., Haehnel, R. B., Sturm, M., Hiemstra, C. A., Berezovskaya, S., and Tabler, R. D.:
998 Instruments and Methods
999 <http://pub2web.metastore.ingenta.com/ns/>
999 Simulating complex snow distributions in windy environments using SnowTran-3D, *Journal of*
000 *Glaciology*, 53, 241-256, 2007.

001 Lopez-Moreno, J. I., Fassnacht, S. R., Begueria, S., and Latron, J.: Variability of snow depth at
002 the plot scale: implications for mean depth estimation and sampling strategies, 2011. 2011.

003 López-Moreno, J. I., Revuelto, J., Fassnacht, S. R., Azorín-Molina, C., Vicente-Serrano, S. M.,
004 Morán-Tejeda, E., and Sexstone, G. A.: Snowpack variability across various spatio-temporal
005 resolutions, *Hydrological Processes*, doi: 10.1002/hyp.10245, 2014. n/a-n/a, 2014.

006 Luce, C. H., Tarboton, D. G., and Cooley, K. R.: The influence of the spatial distribution of snow
007 on basin-averaged snowmelt, *Hydrological Processes*, 12, 1671-1683, 1998.

008 Lundquist, J. D. and Dettinger, M. D.: How snowpack heterogeneity affects diurnal streamflow
009 timing, *Water Resources Research*, 41, W05007, 2005.

010 | Matthews, H. D., Eby, M., Ewen, T., Friedlingstein, P., and Hawkins, B. J.: What determines the
011 magnitude of carbon cycle-climate feedbacks?, *Global Biogeochemical Cycles*, 21, n/a-n/a,
012 2007a.

013 Matthews, H. D., Eby, M., Ewen, T., Friedlingstein, P., and Hawkins, B. J.: What determines the
014 magnitude of carbon cycle-climate feedbacks?, *Global Biogeochemical Cycles*, 21, GB2012,
015 2007b.

016 Matthews, H. D., Weaver, A. J., and Meissner, K. J.: Terrestrial Carbon Cycle Dynamics under
017 Recent and Future Climate Change, *Journal of Climate*, 18, 1609-1628, 2005.

018 McFadden, J. P., Chapin, F. S., and Hollinger, D. Y.: Subgrid-scale variability in the surface
019 energy balance of arctic tundra, *Journal of Geophysical Research: Atmospheres*, 103, 28947-
020 28961, 1998.

021 McGuire, A. D., Clein, J. S., Melillo, J. M., Kicklighter, D. W., Meier, R. A., Vorosmarty, C. J.,
022 and Serreze, M. C.: Modelling carbon responses of tundra ecosystems to historical and projected
023 climate: sensitivity of pan-Arctic carbon storage to temporal and spatial variation in climate,
024 *Global Change Biology*, 6, 141-159, 2000.

025 Mefford, T. K., Bieniulis, M., Halter, B., and Peterson, J.: *Meteorological Measurements*, 17 pp.,
026 1996.

027 Miller, P. C., Stoner, W. A., and Tieszen, L. L.: A Model of Stand Photosynthesis for the Wet
028 Meadow Tundra at Barrow, Alaska, *Ecology*, 57, 411-430, 1976.

029 | [Montaldo, N. and Albertson, J. D.: Temporal dynamics of soil moisture variability: 2.](#)
030 [Implications for land surface models, *Water Resources Research*, 39, n/a-n/a, 2003.](#)

031 Morgner, E., Elberling, B., Strebel, D., and Cooper, E. J.: The importance of winter in annual
032 ecosystem respiration in the High Arctic: effects of snow depth in two vegetation types, *Polar*
033 *Research*, 29, 58-74, 2010.

034 Nobrega, S. and Grogan, P.: Deeper Snow Enhances Winter Respiration from Both Plant-
035 associated and Bulk Soil Carbon Pools in Birch Hummock Tundra, *Ecosystems*, 10, 419-431,
036 2007.

037 Oberbauer, S. F., Tenhunen, J. D., and Reynolds, J. F.: Environmental Effects on CO₂ Efflux
038 from Water Track and Tussock Tundra in Arctic Alaska, U.S.A, *Arctic and Alpine Research*, 23,
039 162-169, 1991.

Gautam Bisht 8/23/2017 5:29 AM

Deleted: Mack, M. C., Schuur, E. A. G., Bret-Harte, M. S., Shaver, G. R., and Chapin, F. S.: Ecosystem carbon storage in arctic tundra reduced by long-term nutrient fertilization, *Nature*, 431, 440-443, 2004. .

045 Oechel, W. C., Hastings, S. J., Vourlitis, G., Jenkins, M., Riechers, G., and Grulke, N.: Recent
046 change of Arctic tundra ecosystems from a net carbon dioxide sink to a source, *Nature*, 361, 520-
047 523, 1993.

048 Oleson, K. W., D.M. Lawrence, G.B. Bonan, B. Drewniak, M. Huang, C.D. Koven, S. Levis, F.
049 Li, W.J. Riley, Z.M. Subin, S.C. Swenson, P.E. Thornton, A. Bozbiyik, R. Fisher, E. Kluzek, J.-
050 F. Lamarque, P.J. Lawrence, L.R. Leung, W. Lipscomb, S. Muszala, D.M. Ricciuto, W. Sacks,
051 Y. Sun, J. Tang, Z.-L. Yang: Technical Description of version 4.5 of the Community Land
052 Model (CLM), National Center for Atmospheric Research, Boulder, CO, 2013a.

053 Oleson, K. W., D.M. Lawrence, G.B. Bonan, B. Drewniak, M. Huang, C.D. Koven, S. Levis, F.
054 Li, W.J. Riley, Z.M. Subin, S.C. Swenson, P.E. Thornton, A. Bozbiyik, R. Fisher, E. Kluzek, J.-
055 F. Lamarque, P.J. Lawrence, L.R. Leung, W. Lipscomb, S. Muszala, D.M. Ricciuto, W. Sacks,
056 Y. Sun, J. Tang, Z.-L. Yang: Technical Description of version 4.5 of the Community Land
057 Model (CLM), National Center for Atmospheric Research, Boulder, CO, [422 pp.](#), 2013b.

058 [Pau, G. S. H., Bisht, G., and Riley, W. J.: A reduced-order modeling approach to represent
059 subgrid-scale hydrological dynamics for land-surface simulations: application in a polygonal
060 tundra landscape, *Geosci. Model Dev.*, 7, 2091-2105, 2014.](#)

061 Randerson, J. T., Lindsay, K., Munoz, E., Fu, W., Moore, J. K., Hoffman, F. M., Mahowald, N.
062 M., and Doney, S. C.: Multicentury changes in ocean and land contributions to the climate-
063 carbon feedback, *Global Biogeochemical Cycles*, 29, 744-759, 2015.

064 Rogers, M. C., Sullivan, P. F., and Welker, J. M.: Evidence of Nonlinearity in the Response of
065 Net Ecosystem CO₂ Exchange to Increasing Levels of Winter Snow Depth in the High Arctic of
066 Northwest Greenland, *Arctic, Antarctic, and Alpine Research*, 43, 95-106, 2011.

067 Rohrbough, J. A., Davis, D. R., and Bales, R. C.: Spatial variability of snow chemistry in an
068 alpine snowpack, southern Wyoming, *Water Resources Research*, 39, 1190, 2003.

069 Schaefer, K., Zhang, T., Bruhwiler, L., and Barrett, A. P.: Amount and timing of permafrost
070 carbon release in response to climate warming, *Tellus B*, 63, 165-180, 2011.

071 Schimel, J. P., Bilbrough, C., and Welker, J. M.: Increased snow depth affects microbial activity
072 and nitrogen mineralization in two Arctic tundra communities, *Soil Biology and Biochemistry*,
073 36, 217-227, 2004.

074 Schuur, E. A. G. and Abbott, B.: Climate change: High risk of permafrost thaw, *Nature*, 480, 32-
075 33, 2011.

Gautam Bisht 8/23/2017 5:29 AM

Deleted: 422 pp.,

Gautam Bisht 8/23/2017 5:29 AM

Deleted: Schimel, J. P., Kielland, K., and Chapin, F. S., III: Nutrient Availability and Uptake by Tundra Plants. In: *Landscape Function and Disturbance in Arctic Tundra*, Reynolds, J. and Tenhunen, J. (Eds.), Ecological Studies, Springer Berlin Heidelberg, 1996. -

084 Schuur, E. A. G., Bockheim, J., Canadell, J. G., Euskirchen, E., Field, C. B., Goryachkin, S. V.,
085 Hagemann, S., Kuhry, P., Lafleur, P. M., Lee, H., Mazhitova, G., Nelson, F. E., Rinke, A.,
086 Romanovsky, V. E., Shiklomanov, N., Tarnocai, C., Venevsky, S., Vogel, J. G., and Zimov, S.
087 A.: Vulnerability of Permafrost Carbon to Climate Change: Implications for the Global Carbon
088 Cycle, *BioScience*, 58, 701-714, 2008.

089 Seppala, M., Gray, J., and Ricard, J.: Development of low-centred ice-wedge polygons in the
090 northernmost Ungava Peninsular, Québec, Canada, *Boreas*, 20, 259-285, 1991.

091 Sexstone, G. A. and Fassnacht, S. R.: What drives basin scale spatial variability of snowpack
092 properties in northern Colorado?, *The Cryosphere*, 8, 329-344, 2014.

093 Sitch, S., Huntingford, C., Gedney, N., Levy, P. E., Lomas, M., Piao, S. L., Betts, R., Ciais, P.,
094 Cox, P., Friedlingstein, P., Jones, C. D., Prentice, I. C., and Woodward, F. I.: Evaluation of the
095 terrestrial carbon cycle, future plant geography and climate-carbon cycle feedbacks using five
096 Dynamic Global Vegetation Models (DGVMs), *Global Change Biology*, 14, 2015-2039, 2008.

097 Smith, L. C., Sheng, Y., MacDonald, G. M., and Hinzman, L. D.: Disappearing Arctic Lakes,
098 *Science*, 308, 1429-1429, 2005.

099 Smith, [M. B.](#), [Koren, V.](#), [Reed, S.](#), [Zhang, Z.](#), [Zhang, Y.](#), [Moreda, F.](#), [Cui, Z.](#), [Mizukami, N.](#),
100 [Anderson, E. A.](#), and [Cosgrove, B. A.](#): [The distributed model intercomparison project – Phase 2:](#)
101 [Motivation and design of the Oklahoma experiments](#), *Journal of Hydrology*, 418, 3-16, 2012.

102 [Smith, N. V.](#), Saatchi, S. S., and Randerson, J. T.: Trends in high northern latitude soil freeze and
103 thaw cycles from 1988 to 2002, *Journal of Geophysical Research: Atmospheres*, 109, D12101,
104 2004.

105 Sturm, M., Douglas, T., Racine, C., and Liston, G. E.: Changing snow and shrub conditions
106 affect albedo with global implications, *Journal of Geophysical Research: Biogeosciences*, 110,
107 G01004, 2005.

108 Sullivan, P.: Snow distribution, soil temperature and late winter CO₂ efflux from soils near the
109 Arctic treeline in northwest Alaska, *Biogeochemistry*, 99, 65-77, 2010.

110 Swenson, S. C. and Lawrence, D. M.: A new fractional snow-covered area parameterization for
111 the Community Land Model and its effect on the surface energy balance, *Journal of Geophysical*
112 *Research: Atmospheres*, 117, n/a-n/a, 2012.

Gautam Bisht 8/23/2017 5:29 AM

Deleted: Shaver, G. and Chapin III, F.:
Effect of fertilizer on production and biomass
of tussock tundra, Alaska, USA, *Arctic and*
Alpine Research, 1986. 261-268, 1986. ... [3]

118 Tang, J. and Riley, W. J.: Large uncertainty in ecosystem carbon dynamics resulting from
119 ambiguous numerical coupling of carbon and nitrogen biogeochemistry: A demonstration with
120 the ACME land model, *Biogeosciences Discuss.*, 2016, 1-27, 2016.

121 Tarnocai, C., Canadell, J. G., Schuur, E. A. G., Kuhry, P., Mazhitova, G., and Zimov, S.: Soil
122 organic carbon pools in the northern circumpolar permafrost region, *Global Biogeochemical*
123 *Cycles*, 23, GB2023, 2009.

124 Thompson, S. L., Govindasamy, B., Mirin, A., Caldeira, K., Delire, C., Milovich, J., Wickett,
125 M., and Erickson, D.: Quantifying the effects of CO₂-fertilized vegetation on future global
126 climate and carbon dynamics, *Geophysical Research Letters*, 31, L23211, 2004.

127 Wadham, J. L., Hallam, K. R., Hawkins, J., and O'Connor, A.: Enhancement of snowpack
128 inorganic nitrogen by aerosol debris, *Tellus B*, 58, 229-241, 2006.

129 Wahren, C. H. A., Walker, M. D., and Bret-Harte, M. S.: Vegetation responses in Alaskan arctic
130 tundra after 8 years of a summer warming and winter snow manipulation experiment, *Global*
131 *Change Biology*, 11, 537-552, 2005.

132 Wainwright, H. M., Dafflon, B., Smith, L. J., Hahn, M. S., Curtis, J. B., Wu, Y., Ulrich, C.,
133 Peterson, J. E., Torn, M. S., and Hubbard, S. S.: Identifying multiscale zonation and assessing
134 the relative importance of polygon geomorphology on carbon fluxes in an Arctic tundra
135 ecosystem, *Journal of Geophysical Research: Biogeosciences*, 120, 788-808, 2015.

136 Walker, D. A., Raynolds, M. K., Daniëls, F. J. A., Einarsson, E., Elvebakk, A., Gould, W. A.,
137 Katenin, A. E., Kholod, S. S., Markon, C. J., Melnikov, E. S., Moskalenko, N. G., Talbot, S. S.,
138 Yurtsev, B. A., and The other members of the, C. T.: The Circumpolar Arctic vegetation map,
139 *Journal of Vegetation Science*, 16, 267-282, 2005.

140 Warscher, M., Strasser, U., Kraller, G., Marke, T., Franz, H., and Kunstmann, H.: Performance
141 of complex snow cover descriptions in a distributed hydrological model system: A case study for
142 the high Alpine terrain of the Berchtesgaden Alps, *Water Resources Research*, 49, 2619-2637,
143 2013.

144 Welker, J. M., Fahnestock, J. T., and Jones, M. H.: Annual CO₂ Flux in Dry and Moist Arctic
145 Tundra: Field Responses to Increases in Summer Temperatures and Winter Snow Depth,
146 *Climatic Change*, 44, 139-150, 2000.

147 Wiggins, I. L.: The distribution of vascular plants on polygonal ground near Point Barrow,
148 Alaska, *Stanford University Contributions of the Dudley Herbarium*, 4, 41-52, 1951.

Gautam Bisht 8/23/2017 5:29 AM

Deleted: Van Wijk, M. T., Clemmensen, K. E., Shaver, G. R., Williams, M., Callaghan, T. V., Chapin, F. S., Cornelissen, J. H. C., Gough, L., Hobbie, S. E., Jonasson, S., Lee, J. A., Michelsen, A., Press, M. C., Richardson, S. J., and Rueth, H.: Long-term ecosystem level experiments at Toolik Lake, Alaska, and at Abisko, Northern Sweden: generalizations and differences in ecosystem and plant type responses to global change, *Global Change Biology*, 10, 105-123, 2004. .

Gautam Bisht 8/23/2017 5:29 AM

Deleted: Walker, M. D., Wahren, C. H., Hollister, R. D., Henry, G. H. R., Ahlquist, L. E., Alatalo, J. M., Bret-Harte, M. S., Calef, M. P., Callaghan, T. V., Carroll, A. B., Epstein, H. E., Jónsdóttir, I. S., Klein, J. A., Magnússon, B., Molau, U., Oberbauer, S. F., Rewa, S. P., Robinson, C. H., Shaver, G. R., Suding, K. N., Thompson, C. C., Tolvanen, A., Totland, Ø., Turner, P. L., Tweedie, C. E., Webber, P. J., and Wookey, P. A.: Plant community responses to experimental warming across the tundra biome, *Proceedings of the National Academy of Sciences of the United States of America*, 103, 1342-1346, 2006. .

174 Williams, M. W., Hood, E., and Caine, N.: Role of organic nitrogen in the nitrogen cycle of a
175 high-elevation catchment, Colorado Front Range, *Water Resources Research*, 37, 2569-2581,
176 2001.

177 Williams, T. and Flanagan, L.: Effect of changes in water content on photosynthesis,
178 transpiration and discrimination against $^{13}\text{CO}_2$ and $\text{C}^{18}\text{O}^{16}\text{O}$ in *Pleurozium* and *Sphagnum*,
179 *Oecologia*, 108, 38-46, 1996.

180 Wu, Y., Hubbard, S. S., Ulrich, C., and Wulfschleger, S. D.: Remote Monitoring of Freeze-
181 Thaw Transitions in Arctic Soils Using the Complex Resistivity Method, *gsvadzone*, 2013. 2013.

182 Xu, X., Riley, W. J., Koven, C. D., Billesbach, D. P., Chang, R. Y. W., Commane, R.,
183 Euskirchen, E. S., Hartery, S., Harazono, Y., Iwata, H., McDonald, K. C., Miller, C. E., Oechel,
184 W. C., Poulter, B., Raz-Yaseef, N., Sweeney, C., Torn, M., Wofsy, S. C., Zhang, Z., and Zona,
185 D.: A multi-scale comparison of modeled and observed seasonal methane emissions in northern
186 wetlands, *Biogeosciences*, 13, 5043-5056, 2016.

187 Zeng, N., Qian, H., Munoz, E., and Iacono, R.: How strong is carbon cycle-climate feedback
188 under global warming?, *Geophysical Research Letters*, 31, L20203, 2004.

189 Zeng, X. and Decker, M.: Improving the Numerical Solution of Soil Moisture-Based Richards
190 Equation for Land Models with a Deep or Shallow Water Table, *Journal of Hydrometeorology*,
191 10, 308-319, 2009.

192 Zhu, Q., Iversen, C. M., Riley, W. J., Slette, I. J., and Vander Stel, H. M.: Root traits explain
193 observed tundra vegetation nitrogen uptake patterns: Implications for trait-based land models,
194 *Journal of Geophysical Research: Biogeosciences*, 121, 3101-3112, 2016.

195 Zhu, Q. and Riley, W. J.: Improved modelling of soil nitrogen losses, *Nature Clim. Change*, 5,
196 705-706, 2015.

197 Zona, D., Lipson, D. A., Zulueta, R. C., Oberbauer, S. F., and Oechel, W. C.: Microtopographic
198 controls on ecosystem functioning in the Arctic Coastal Plain, *Journal of Geophysical Research:*
199 *Biogeosciences*, 116, G00I08, 2011.

200

Gautam Bisht 8/23/2017 5:29 AM

Deleted: Wilmking, M., Juday, G. P., Barber, V. A., and Zald, H. S. J.: Recent climate warming forces contrasting growth responses of white spruce at treeline in Alaska through temperature thresholds, *Global Change Biology*, 10, 1724-1736, 2004. .

Gautam Bisht 8/23/2017 5:29 AM

Deleted: 2016a

Gautam Bisht 8/23/2017 5:29 AM

Deleted: Zhu, Q., Riley, W. J., Tang, J., and Koven, C. D.: Multiple soil nutrient competition between plants, microbes, and mineral surfaces: model development, parameterization, and example applications in several tropical forests, *Biogeosciences*, 13, 341-363, 2016b. .

Gautam Bisht 8/23/2017 5:29 AM

Deleted: .